

Translating ferroptosis into oncology: challenges, opportunities and future directions

Rui Kang¹✉, Jiao Liu²✉, Jiayi Wang^{3,4}✉, Guido Kroemer^{5,6,7}✉ & Daolin Tang¹✉

Abstract

Ferroptosis is an oxidative, lipid peroxidation-driven form of regulated cell death that occurs when antioxidant and organelle-protective systems are compromised. Increasing evidence implicates ferroptosis as a process that can exert both tumour-suppressive and tumour-promoting effects depending on cellular context at multiple stages of cancer evolution (from tumour initiation to metastatic colonization), sparking substantial interest in therapeutically exploiting this mechanism of cell death. Yet, despite rapid preclinical progress, clinical translation of ferroptosis-based strategies remains nascent. In this Review, we examine the major barriers to translation, including pharmacological limitations, tumour-intrinsic heterogeneity, microenvironmental and immune constraints, and gaps in current preclinical modelling. We also highlight emerging opportunities such as new ferroptosis-inducing agents, biomarker-guided patient selection and rational combinations with chemotherapy, radiotherapy, targeted agents or immunotherapies. Finally, we outline a translational roadmap for integrating ferroptosis-based therapies into oncology practice. By defining key challenges and future directions, this Review aims to position ferroptosis as a viable therapeutic paradigm and to accelerate progress towards clinical application.

Sections

Introduction

Core mechanisms of ferroptosis in cancer cells

Challenges for clinical translation

Opportunities and emerging solutions

Roadmap for clinical translation

Conclusions

¹Department of Surgery, UT Southwestern Medical Center, Dallas, TX, USA. ²DAMP Laboratory, Third Affiliated Hospital of Guangzhou Medical University, Guangzhou, China. ³Department of Clinical Laboratory, Shanghai Chest Hospital, Shanghai Jiao Tong University School of Medicine, Shanghai, China. ⁴Shanghai Institute of Thoracic Oncology, Shanghai Chest Hospital, Shanghai Jiao Tong University School of Medicine, Shanghai, China. ⁵INSERM U1138, Equipe labellisée par la Ligue contre le cancer, Centre de Recherche des Cordeliers, Université Paris Cité, Sorbonne Université, Paris, France. ⁶Metabolomics and Cell Biology Platforms, UMS AMMiCa, Institut Gustave Roussy, INSERM US23/CNRS UAR 3655, Université Paris-Saclay, Villejuif, France. ⁷Institut du Cancer Paris CARPEM, Department of Biology, Hôpital Européen Georges Pompidou, AP-HP, Paris, France. ✉e-mail: rui.kang@utsouthwestern.edu; 2018683073@gzhmu.edu.cn; jiayi.wang@sjtu.edu.cn; kroemer@orange.fr; daolin.tang@utsouthwestern.edu

Key points

- Ferroptosis is a lipid peroxidation-driven cell death process shaped by antioxidant, metabolic and organelle-protective pathways, highlighting the adaptive plasticity that cancer cells use to maintain redox homeostasis.
- Tumour-intrinsic heterogeneity, including variable genetic, metabolic, epigenetic and lineage programmes, creates diverse ferroptosis sensitivities, reinforcing the need for biomarker-guided patient selection rather than uniform therapeutic strategies.
- The tumour microenvironment, including stromal buffering, hypoxia, acidosis, immune cell vulnerability and microbiota-derived metabolites, profoundly modulates ferroptosis, making therapeutic induction inherently context dependent.
- First-generation ferroptosis inducers have limited drug-like properties, whereas new agents, including GPX4 and FSP1 inhibitors, degraders, prodrugs, nanocarriers and antibody–drug conjugates, offer improved potency and tumour selectivity.
- Integrated genomic, transcriptomic, lipidomic and imaging biomarkers, including ACSL4, TFRC, various damage-associated molecular patterns and ferroptosis-focused PET probes, are essential for predicting ferroptosis sensitivity and pharmacodynamic monitoring pathway modulation.
- Rational combinations of ferroptosis inducers with immunotherapy, radiotherapy, targeted therapies and metabolic inhibitors can exploit ferroptosis vulnerabilities to overcome therapeutic resistance and improve efficacy but require careful calibration to avoid immune or non-malignant tissue toxicity.

Introduction

Despite major advances in surgery, radiotherapy, targeted therapy and immunotherapy, selective eradication of malignant cells while preserving non-malignant tissues – the central goal of medical oncology – remains challenging. Conventional non-surgical therapies, particularly pharmacological treatments, have largely been conceived as inducers of apoptosis; however, the recognition that cancer cells can evade apoptosis has catalysed growing interest in exploiting alternative, non-apoptotic cell death pathways¹. Among these pathways, ferroptosis – first uncovered via synthetic lethal compound screening that revealed a metabolic vulnerability in BJ-TERT/LT/ST/RAS^{V12}-transformed human foreskin fibroblasts² – has emerged as a mechanistically distinct form of regulated cell death with increasing translational relevance³.

Ferroptosis is defined by the unchecked accumulation of phospholipid hydroperoxides (PLOOH) that compromise the integrity of membranes surrounding cells and organelles⁴. Reduction–oxidation (redox)-active iron and Fenton chemistry are considered core drivers of ferroptosis, although metabolic stresses such as copper overload⁵ and certain photosensitizers used for photodynamic therapy⁶ can trigger ferroptotic cancer cell death through partially iron-independent mechanisms, prompting renewed discussion about the biochemical boundaries of ferroptosis. Nevertheless, dysregulated lipid metabolism and perturbed iron handling remain the most consistent molecular

hallmarks of ferroptosis⁷. Unlike apoptosis, ferroptosis proceeds independently of caspase activation, yet intersects with apoptotic signalling through shared regulatory nodes. For example, after being released from disrupted mitochondria, cytosolic cytochrome *c* (CYCS) promotes apoptosis by triggering assembly of the CYCS–apoptotic peptidase activating factor 1 (APAF1)–caspase 9 (CASP9) apoptosome, but suppresses ferroptosis by forming a CYCS–inositol polyphosphate-4-phosphatase type IA (INPP4A) complex that enhances INPP4A activity, thereby increasing phosphatidylinositol-3-phosphate levels and preventing phospholipid peroxidation⁸. By contrast, BCL-2-like protein 11 (BCL2L11; also known as BIM) and BCL2L4 (more commonly known as BAX) are classic initiators of mitochondrial apoptosis but can also promote downregulation of solute carrier family 7 member 11 (SLC7A11) and glutathione (GSH) peroxidase 4 (GPX4) at the protein level via mechanisms that remain incompletely defined⁹. This activity enhances PLOOH-driven ferroptosis, thus linking mitochondrial outer membrane permeabilization to both apoptotic and ferroptotic cell death programmes⁹. Importantly, ferroptosis induction provides a potential strategy to eradicate chemotherapy-tolerant persister cancer cells, which frequently emerge by acquiring resistance to apoptosis^{10,11}.

Cancer biology has become the dominant arena for ferroptosis research, reflecting the strong influence of oncogenic signalling, redox metabolism and membrane lipid composition on ferroptosis sensitivity, as well as the rapid development of chemical inducers of ferroptosis, which have shown preclinical promise alone or in combination with existing anticancer therapies^{12,13}. More than 20,000 ferroptosis-related studies have been published in the past 5 years – over half with a focus on cancer – and yet clinical translation has lagged. Only a small number of ferroptosis-modulating agents have entered early-phase clinical trials, and none has progressed to routine clinical use.

In this Review, we address a central and timely question for the oncology community: why ferroptosis, despite its clear mechanistic appeal, has not yet been successfully exploited for the treatment of patients with cancer. We examine the conceptual, pharmacological and translational barriers that have impeded progress and outline strategies to overcome them. By illuminating these obstacles and proposing a roadmap for next-generation therapeutic development, we aim to facilitate the evolution of ferroptosis from a compelling biological concept to a clinically actionable anticancer mechanism.

Core mechanisms of ferroptosis in cancer cells

Ferroptosis is a form of oxidative cell death that arises when the cellular capacity to detoxify PLOOH is exceeded, leading to progressive membrane damage (Fig. 1). Because reactive oxygen species (ROS) are a natural by-product of aerobic metabolism, cells have evolved multilayered antioxidant systems to suppress lipid peroxidation and preserve membrane integrity. In cancer cells, these antioxidant defences can be broadly categorized into GPX4-dependent and GPX4-independent pathways, which together establish the threshold for ferroptosis induction and provide a conceptual framework for the mechanisms discussed below.

In addition to synthetic radical-trapping antioxidants (RTAs) such as ferrostatin 1 (ref. 3) and liproxstatin 1 (ref. 14), which are often used to suppress ferroptosis in studies investigating this form of cell death, numerous endogenous RTAs can terminate phospholipid radical propagation, including vitamin E³, reduced coenzyme Q (CoQH₂)^{15–17}, tetrahydrobiopterin^{18,19}, vitamin K^{20,21}, hydropersulfides²² and serotonin²³. These diverse defence systems underscore the strong evolutionary pressure to constrain lipid peroxidation-driven damage

and highlight the remarkable plasticity of cancer cells, which readily activate compensatory antioxidant pathways to maintain ferroptosis resistance when a single safeguard is compromised^{15–17}.

At the core of ferroptosis regulation is the GPX4–GSH axis²⁴. The selenoenzyme GPX4 reduces PLOOH to their corresponding alcohols (PLOH) using the glutamate–cysteine–glycine tripeptide GSH as the electron donor²⁴. Early studies of ferroptosis in cancer identified GPX4 as an essential survival factor²⁴. Genetic or pharmacological inhibition of GPX4 causes catastrophic membrane peroxidation and selectively suppresses the growth of multiple tumour types in preclinical models, with particularly pronounced vulnerabilities observed in diffuse large B cell lymphomas and renal cell carcinomas^{24,25}. The subcellular localization, post-translational regulation and proteostatic control of GPX4 are stringently coordinated²⁶, collectively setting different ferroptosis thresholds (Fig. 2 and Box 1).

GSH production largely depends on system xc⁻, a heterodimeric cystine–glutamate antiporter composed of the transporter subunit SLC7A11 and the glycoprotein subunit SLC3A2: this complex mediates cellular uptake of cystine, which can then be reduced to cysteine and used for GSH biosynthesis. Genetic deletion of *Slc7a11* or dietary cystine restriction induces ferroptosis-mediated tumour suppression in mouse models such as oncogenic *Kras*-driven and *Tp53*-mutant pancreatic ductal adenocarcinoma (PDAC), underscoring the profound reliance of tumour development on sustained cysteine supply²⁷. Beyond its canonical plasma membrane-related role, SLC7A11 also localizes to lysosomes, where it functions as an H⁺ antiporter; its loss causes lysosomal hyperacidification, impaired proteolysis and ferroptotic death – highlighting a previously unappreciated organelle-specific dimension of cystine metabolism²⁸.

A major GPX4-independent protective pathway is mediated by ferroptosis suppressor protein 1 (FSP1; also known as AIFM2). FSP1 is an NAD(P)H-dependent oxidoreductase that reduces CoQ₁₀ to its radical-trapping form CoQH₂ (refs. 15,16) (Fig. 1). Myristoylation of FSP1 is essential for membrane anchoring of this enzyme, thereby positioning FSP1 and thus CoQH₂ to intercept lipid peroxyl radicals at the plasma membrane and other non-mitochondrial sites^{15,16}. This pathway becomes particularly important in GPX4-low or GPX4-null cancer cells, in which FSP1 functions as a compensatory antioxidant system^{15,16}. The activity of FSP1 is further supported by aldehyde dehydrogenase (ALDH) 7 family member A1 (ALDH7A1)-derived membrane NADH pools, with AMP-activated protein kinase (AMPK) recruiting ALDH7A1 to cell membranes under ferroptotic stress to stabilize FSP1 (ref. 29). Additionally, FSP1 reduces vitamin K to its active hydroquinone form (VKH₂)²⁰ and supports endosomal sorting complexes for transport III (ESCRT-III)-mediated plasma membrane repair³⁰ (Fig. 1) – two stress-adaptive processes that are frequently upregulated in therapy-resistant cancers, including hepatocellular carcinoma (HCC). FSP1 also localizes to the membranes of lipid droplets and lysosomes, thereby mitigating organelle-specific ferroptotic damage^{31,32} (Fig. 2b). Collectively, these activities position FSP1 as an important coordinator of membrane repair pathways and antioxidant defence pathways. How cancer cells dynamically prioritize these diverse functions of FSP1 under therapeutic stress remains an important open question.

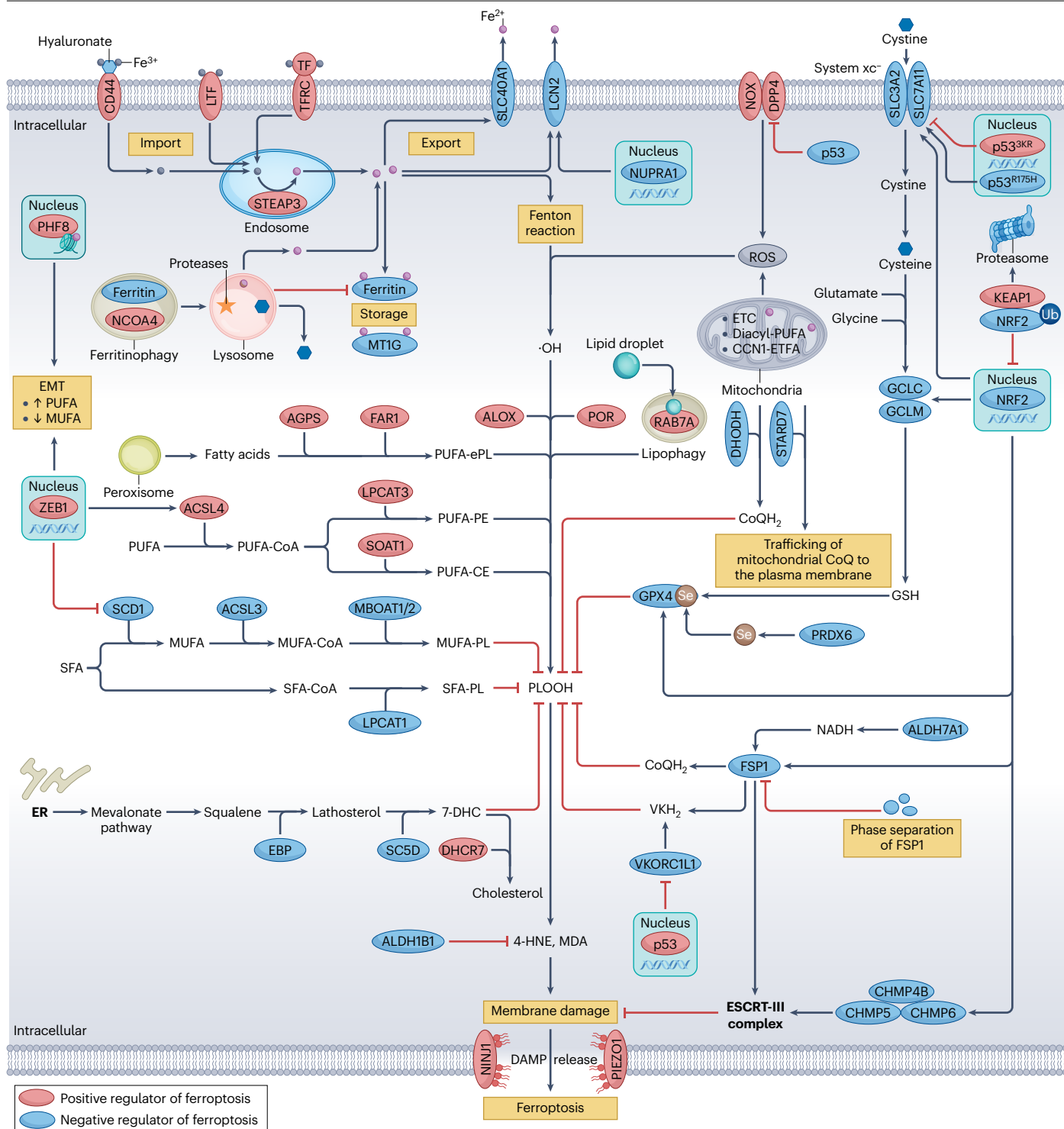
Notably, both GPX4-dependent and GPX4-independent antioxidant systems converge on nuclear factor erythroid 2-related factor 2 (NRF2; also known as NFE2L2), which coordinates the expression of *SLC7A11*, *GPX4* and *AIFM2* (FSP1), as well as genes encoding GSH biosynthetic enzymes (*GCLC* and *GCLM*), metallothioneins (for example, *MT1G*) and components of broader detoxification pathways^{33–36} (Fig. 1).

This convergence highlights NRF2 as a central transcriptional integrator of ferroptosis resistance, thus suggesting that its modulation might exert broader effects than targeting individual downstream effectors.

Iron metabolism is another key determinant of ferroptosis (Fig. 1). Redox-active Fe²⁺ fuels Fenton chemistry to produce ROS and enables the activity of iron-dependent lipid peroxidases, such as lipoxygenases and cytochrome P450 oxidoreductase (POR)^{37,38}. Many tumours have expanded labile iron pools (LIPs) owing to elevated expression of the transferrin receptor (TFRC; also known as TfR1), increased autophagic degradation of the iron-storage protein ferritin (ferritinophagy), altered haem turnover and impaired mitochondrial iron–sulfur cluster synthesis, collectively increasing ferroptotic susceptibility^{39,40}. Beyond TFRC, alternative iron uptake routes also contribute to this LIP expansion. For example, CD44 promotes hyaluronate-bound iron endocytosis, thereby driving epithelial–mesenchymal transition (EMT) via epigenetic reprogramming mediated by the nuclear iron-dependent histone lysine demethylase PHF8 (ref. 41), and the resulting therapy-resistant mesenchymal cancer cells consequently exhibit heightened sensitivity to lipid peroxidation^{10,11}. By contrast, lactotransferrin (LTF)-dependent iron import is restrained by NEDD4-like E3 ubiquitin protein ligase (NEDD4L)-driven proteasomal degradation of LTF in PDAC cell lines, thereby limiting LIP expansion and ferroptosis⁴². Conversely, the iron exporter ferroportin 1 (also known as SLC40A1) restricts intracellular Fe²⁺ accumulation, and its autophagic degradation expands the LIP and thus promotes ferroptosis in various cancer cell lines and in mouse models of PDAC⁴³. Additional iron-sequestration pathways, such as nuclear protein 1 (NUPR1)-dependent transcriptional upregulation of the iron-trafficking protein lipocalin 2 (LCN2) in PDAC and aged lung epithelium (and thus ageing-associated lung adenocarcinomas), limit iron availability and suppress ferroptosis^{44,45}. The metal cation symporter ZIP14 (also known as SLC39A14) has also been implicated in iron transport linking ferroptosis to systemic iron homeostasis, primarily in liver injury models⁴⁶. Notably, ferritinophagy mediated by the autophagic ferritin receptor, nuclear receptor coactivator 4 (NCOA4), remains the predominant mechanism by which cancer cells expand their LIP and, consequently, have an increased susceptibility to ferroptotic cell death^{39,40}.

Lipid pathway reprogramming further dictates ferroptosis sensitivity (Fig. 1). Polyunsaturated fatty acid (PUFA)-containing phospholipids (PUFA-PLs) generated by long-chain fatty acid CoA ligase 4 (ACSL4; also known as LACS4) and lysophosphatidylcholine acyltransferase 3 (LPCAT3) are the core substrates for lethal lipid peroxidation, and their enrichment in several aggressive cancers confers ferroptotic sensitivity^{47–49}. Notably, ACSL4 consistently emerges as one of the top ferroptosis determinants across independent genome-wide CRISPR–Cas9 screens in diverse cancers^{25,48,50}, underscoring its central role as a robust promoter of ferroptosis. By contrast, stearoyl-CoA desaturase (SCD1)–ACSL3-driven monounsaturated fatty acid (MUFA)-containing phospholipid (MUFA-PL) synthesis^{51,52} and LPCAT1-dependent generation of saturated fatty acid phospholipids (SFA-PLs)⁵³ suppress ferroptosis in cancers such as HCC. In addition, the lipid flippase SLC47A1 (also known as MATE1) functions as an endogenous suppressor of ferroptosis across multiple cancer types by limiting intracellular docosahexaenoic acid and docosapentaenoic acid accumulation and preventing ACSL4–sterol O-acyltransferase 1 (SOAT1)-dependent PUFA-containing cholesteryl ester (PUFA-CE) formation, thereby reducing lipid peroxidation⁵⁴. Thus, the balance between PUFA-containing and MUFA-containing membrane lipids is a key metabolic rheostat governing ferroptotic vulnerability.

Review article



Multiple organelles cooperate to regulate the initiation and execution of ferroptosis (Fig. 1). Mitochondria contribute via glutaminolysis-driven tricarboxylic acid cycle flux, electron transport chain (ETC)-derived ROS and iron–sulfur cluster turnover^{55,56}. Diacyl-PUFA-containing phosphatidylcholines (PUFA-PCs) directly interact with ETC complex I and amplify mitochondrial ROS (mtROS)

production, thus establishing an essential mitochondrial component of ferroptosis⁵⁷. Conversely, the presenilin-associated rhomboid-like (PARL)–StAR-related lipid transfer domain-containing protein 7 (STARD7)–CoQ₁₀ axis governs the transport of mitochondrial CoQ₁₀ to the plasma membrane, thereby sustaining a GPX4-independent protective circuit⁵⁸. In addition, although high-dose dihydroorotate

Fig. 1 | Key metabolic, organellar and signalling networks governing ferroptosis in cancer cells. Ferroptosis is initiated by the iron-dependent accumulation of phospholipid hydroperoxides (PLOOH), generated through coordinated metabolic and organelle-derived inputs. Iron homeostasis is shaped by transferrin (TF)–transferrin receptor 1 (TFRC)-mediated import as well as by CD44-dependent and lactotransferrin (LTF)-dependent endocytosis of Fe³⁺, intracellular metalloreductase STEAP3-driven reduction of Fe³⁺ to Fe²⁺, ferritin-mediated storage and metallothionein 1G (MT1G)-mediated chelation, nuclear receptor coactivator 4 (NCOA4)-mediated ferritinophagy, lysosomal turnover, and Fe²⁺ export via solute carrier family 40 member 1 (SLC40A1) and lipocalin 2 (LCN2). Redox-active Fe²⁺ can amplify lipid peroxidation through Fenton chemistry. Lipid metabolic pathways specify substrate availability: long-chain fatty acid CoA ligase 4 (ACSL4) and lysophosphatidylcholine acyltransferase 3 (LPCAT3) drive the synthesis of polyunsaturated fatty acid phospholipids that undergo arachidonate lipoxygenase (ALOX)/cytochrome P450 oxidoreductase (POR)-mediated peroxidation, whereas ACSL3, membrane-bound *O*-acyltransferases 1 and 2 (MBOAT1/2), stearoyl-CoA desaturase (SCD1) and LPCAT1 promote monounsaturated fatty acid (MUFA)-containing phospholipid (MUFA-PL) generation to limit ferroptosis. Peroxisomal alkyl-dihydroxyacetone phosphate synthase (AGPS) and fatty acyl-CoA reductase 1 (FAR1) produce polyunsaturated fatty acid (PUFA)-containing ether phospholipids (PUFA-ePLs) that enhance susceptibility, while sterol *O*-acyltransferase 1 (SOAT1) activity and Ras-related protein RAB7A-dependent lipophagy can further expand oxidizable lipid pools. Mitochondria and NADPH oxidase (NOX) enzymes supply reactive oxygen species (ROS), and mitochondrial coenzyme Q (CoQ) redox cycling and trafficking are governed by mitochondrial dihydroorotate dehydrogenase (DHODH) and StAR-related lipid transfer protein 7 (STARD7). Antioxidant systems counterbalance lipid peroxidation: system xc⁻ supports glutathione (GSH) synthesis under the control of p53 and nuclear factor erythroid 2-related factor 2 (NRF2); glutathione peroxidase 4 (GPX4) detoxifies PLOOH using

GSH; and compartment-specific protection is provided by DHODH-driven and ferroptosis suppressor protein 1 (FSP1)-driven generation of reduced coenzyme Q₁₀ (CoQH₂; also known as ubiquinol) and/or vitamin K hydroquinone (VKH₂). Membrane-associated NADH can be generated by aldehyde dehydrogenase 7 family member A1 (ALDH7A1) and supports both the activity and membrane localization of FSP1. Vitamin K epoxide reductase complex subunit 1-like 1 (VKORC1L1) suppresses ferroptosis via reduction of vitamin K to VKH₂. Transcriptional or epigenetic regulators including p53, nuclear protein 1 (NUPR1), zinc finger E-box-binding homeobox 1 (ZEB1), NRF2 and histone lysine demethylase PHF8 can reprogramme iron handling, redox buffering and lipid composition. Ferroptosis execution involves PLOOH accumulation, generation of toxic aldehydes such as 4-hydroxynonenal (4-HNE) and malondialdehyde (MDA), membrane rupture driven by ninjurin 1 (NINJ1) and/or piezo-type mechanosensitive ion channel component 1 (PIEZO1), and insufficient endosomal sorting complex required for transport-III (ESCRT-III)-mediated membrane repair and impaired aldehyde dehydrogenase 1 family member B1 (ALDH1B1)-dependent PLOOH detoxification. Together, these pathways integrate oncogenic state, metabolic wiring and organelle function to determine ferroptotic susceptibility across cancers. 7-DHC, 7-dehydrocholesterol; CCN1, cellular communication network factor 1; CHMPs, charged multivesicular body proteins; DAMP, damage-associated molecular pattern; DHCR7, 7-DHC reductase; DPP4, dipeptidyl peptidase 4; EBP, emopamil-binding protein; EMT, epithelial–mesenchymal transition; ER, endoplasmic reticulum; ETC, electron transport chain; ETFA, electron transfer flavoprotein subunit- α ; GCLC, glutamate–cysteine ligase catalytic subunit; GCLM, glutamate–cysteine ligase modifier subunit; KEAP1, Kelch-like ECH-associated protein 1; PRDX6, peroxiredoxin 6; PUFA-CE, PUFA-containing cholesteryl esters; PUFA-PE, polyunsaturated phosphatidylethanolamine; SC5D, sterol-C5-desaturase; SFA, saturated fatty acid; SFA-PL, SFA phospholipid; SLC3A2, solute carrier family 3 member 2; SLC7A11, solute carrier family 7 member 11; Ub, ubiquitin.

dehydrogenase (DHODH) inhibitors have been reported to sensitize cancer cells to ferroptosis via off-target effects on FSP1 (ref. 59), DHODH itself catalyses mitochondrial CoQH₂ production, providing a compartment-specific defence that can suppress ferroptosis in GPX4-low cancers¹⁷. Definitive clarification of this mechanism will require systematic comparison of genetic and pharmacological perturbations to resolve on-target versus off-target effects. Mitochondrial iron import and dynamics further modulate ferroptosis sensitivity; for example, iron-triggered mitochondrial translocation of CNN family member 1 (CCN1) facilitates CCN1–electron transfer flavoprotein subunit A (ETF A) complex assembly, thereby promoting fatty acid-dependent mtROS production in models of lung cancer⁶⁰, whereas mitochondrial fusion mediated by dynamin-like GTPase OPA1 or mitofusin 1/2 (MFN1/2) increases susceptibility to ferroptosis by increasing mtROS production in mouse embryonic fibroblasts and human PDAC cell lines^{61,62}. Defining how these mitochondrial circuits integrate with extramitochondrial lipid peroxidation pathways remains a key unmet challenge and will be essential for distinguishing ferroptosis from other cell death modalities, such as apoptosis.

Lysosomes, which are enriched in labile iron, can promote ferroptosis through iron release or selective autophagy – a pathway frequently hyperactivated in cancers^{39,40,63–65} (Fig. 1). By contrast, lysosomal cystine deficiency activates the aryl hydrocarbon receptor (AHR) and in turn activates an activating transcription factor 4 (ATF4)-mediated pathway⁶⁶, whereas lysosomal catabolism of extracellular albumin provides cysteine to fuel cytosolic GSH production in order to sustain redox balance and suppress ferroptosis⁶⁷. Preclinical studies using a lysosome-targeted cysteine-rich fusion construct (termed

CysRx) demonstrate that selective lysosomal cystine stress is sufficient to trigger ferroptosis and suppress tumour growth in vivo⁶⁶. These findings highlight lysosomes as a therapeutically exploitable hub that integrates iron handling, cysteine metabolism and stress-adaptive signalling to govern ferroptosis sensitivity in cancer.

The endoplasmic reticulum (ER) influences ferroptosis through roles in lipid synthesis, unfolded protein response signalling and redox regulation, including the synthesis and intracellular distribution of key antioxidants such as CoQ₁₀ and vitamins⁶⁸. ER–mitochondria contact sites serve as hubs for phospholipid peroxidation in triple-negative breast cancer (TNBC) cells⁶⁹. Peroxisomes can promote ferroptosis by generating PUFA-containing ether phospholipids (PUFA-ePLs) through the coordinated activities of alkyl-dihydroxyacetone phosphate synthase (AGPS) and fatty acyl-CoA reductase 1 (FAR1), which supply highly peroxidizable substrates (Fig. 1); genetic disruption of this PUFA-ePLs axis accelerates tumour growth in xenograft models of ovarian cancer and clear cell renal cell carcinoma (ccRCC) by enabling escape from GPX4 loss-induced ferroptotic pressure⁷⁰. Intracellular lipid droplets can transiently sequester PUFA-containing and MUFA-containing lipids to limit peroxidation, but can also be mobilized through lipophagy to release such substrates to fuel ferroptosis^{31,71} (Fig. 1). Although ferroptosis is executed outside the nucleus, nuclear transcriptional and epigenetic programmes regulate sensitivity to this form of cell death by determining the abundance of pro-ferroptotic and anti-ferroptotic proteins^{33–36}. A key unanswered question is how the organelle crosstalk mediating ferroptotic sensitivity is coordinated, and what are the optimal windows this crosstalk provides to either inhibit or activate ferroptosis.

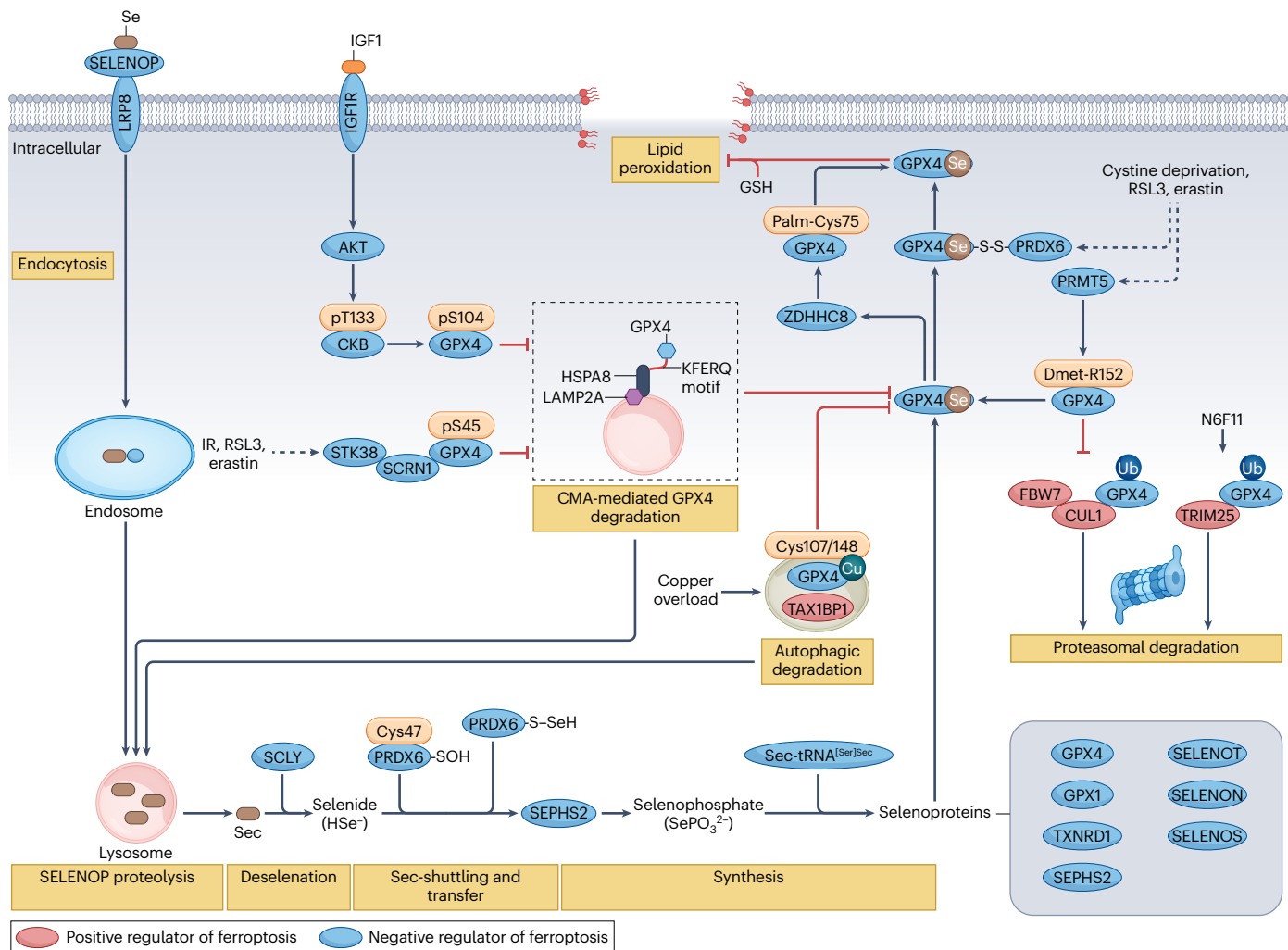


Fig. 2 | Regulation of GPX4 stability and activity in tumour ferroptosis.

Selenoprotein P (SELENOP) delivers selenium to cancer cells through low-density lipoprotein receptor-related protein 8 (LRP8)-mediated endocytosis. Lysosomal proteolysis releases selenocysteine (Sec), which is converted by selenocysteine lyase (SCLY) into selenide (HSe^-). Under oxidative conditions, selenide forms a perselenide (S–SeH) intermediate on residue cysteine 47 (Cys47) of peroxiredoxin 6 (PRDX6), enabling selenium transfer to selenophosphate synthase 2 (SEPHS2) for the generation of selenophosphate (SePO_3^{2-}) and the synthesis of Sec-tRNA^{(Ser)Sec}. The generation of this tRNA supports co-translational production of glutathione peroxidase 4 (GPX4) and other key selenoproteins. GPX4 abundance and activity are shaped by multiple post-translational mechanisms. Insulin-like growth factor 1 (IGF1)–IGF1 receptor (IGF1R)–AKT signalling enhances GPX4 stability through creatine kinase B-type (CKB)-mediated phosphorylation of serine 104 (S104), whereas serine–threonine kinase 38 (STK38) and secernin 1 (SCRN1) phosphorylate GPX4 at additional regulatory sites (including S45). Lipid peroxidation triggers degradation of GPX4 via chaperone-mediated autophagy (CMA) involving lysosome-associated membrane protein 2A (LAMP2A) and heat shock protein family A member 8 (HSPA8); phosphorylation of GPX4 at S45 or S104 suppresses its recognition by HSPA8. Notably, agents that initially induce ferroptotic stress, such as ionizing radiation (IR), the GPX4 inhibitor RSL3 or the cystine–glutamate antiporter (system xc⁻) inhibitor erastin, can indirectly promote formation of

the STK38–SCRN1–GPX4 complex as a compensatory feedback mechanism that limits CMA-mediated GPX4 degradation and might, therefore, contribute to resistance of these agents. By contrast, copper overload promotes TAX1-binding protein 1 (TAX1BP1)-dependent autophagic degradation of GPX4. Palmitoyltransferase ZDHHC8 (ZDHHC8)-mediated S-palmitoylation Cys75 supports the membrane association of GPX4 and ferroptosis resistance, whereas PRDX6 promotes GPX4 disulfide bond formation – which is also required for GPX4 activity and localization to the plasma membrane – as an adaptive response under conditions of cystine deprivation or GPX4 inhibition. Additional negative regulators of ferroptosis include protein arginine methyltransferase 5 (PRMT5), which catalyses arginine 152 demethylation (Dmet-R152) of GPX4 and thereby prevents its F-box/WD repeat-containing protein 7 (FBW7)–cullin 1 (CUL1) ubiquitin ligase-mediated proteasomal degradation; this protective mechanism can also be indirectly upregulated as a compensatory response to cystine deprivation or GPX4 inhibition, thus stabilizing GPX4 and partially counteracting ferroptotic damage. Conversely, the selective ferroptosis inducer N6F11 specifically triggers TRIM25-dependent proteasomal degradation of GPX4. Collectively, these pathways integrate selenium uptake, Sec biosynthesis, post-translational modification and protein quality control to shape GPX4 function and thus ferroptosis sensitivity in cancer cells. GPX1, glutathione peroxidase 1; GSH, glutathione; SELENON, selenoprotein N; SELENOS, selenoprotein S; SELENOT, selenoprotein T; TXNRD1, thioredoxin reductase 1; Ub, ubiquitin.

Box 1 | GPX4 localization and post-translational regulation shape ferroptotic responses in cancer

The ferroptotic threshold in cancer cells is determined largely by the compartment-specific activity of glutathione peroxidase 4 (GPX4) across cytosolic, mitochondrial and nuclear pools, each providing distinct lipid repair functions under metabolic and therapeutic stress. Cytosolic GPX4 has a central role in detoxifying phospholipid hydroperoxides (PLOOH), mitochondrial GPX4 safeguards respiratory chain integrity²⁴³ and nuclear GPX4 can restrict therapy-induced DNA oxidation²⁴⁴, with the relative abundance of each isoform varying substantially across tumour lineages.

GPX4 is further controlled by an extensive post-translational modification (PTM) network that modulates its stability, catalytic efficiency, membrane targeting and degradation (Fig. 2). Incorporation of selenocysteine into GPX4 requires the mevalonate–selenophosphate synthetase 2 (SEPHS2) axis, and peroxiredoxin 6 (PRDX6) facilitates this process through its cysteine 47-dependent selenide shuttling and transfer activity^{245,246}. Via the same residue, PRDX6 can also form a disulfide-linked heterodimer with GPX4 that directs GPX4 to plasma membrane microdomains; disrupting this structural coupling impairs GPX4 localization, increases peroxidation of polyunsaturated fatty acid (PUFA) phospholipid and sensitizes cancer cells to the ferroptosis inducer imidazole ketone erastin (IKE) in mouse xenograft models, including patient-derived hepatocellular carcinoma (HCC) xenografts²⁴⁷.

Phosphorylation of GPX4 provides another dominant stabilizing mechanism. In HCC, secernin 1 (SCRN1) acts as a scaffold for serine–threonine protein kinase 38 (STK38) to phosphorylate GPX4 at serine 45, which blocks recognition of GPX4 by heat shock protein family A member 8 (HSPA8; also known as heat shock cognate 71kDa protein) and lysosome-associated membrane glycoprotein 2A (LAMP2A) that drive chaperone-mediated autophagy (CMA); thus SCRN1 suppresses GPX4 degradation, thereby preventing ferroptosis and driving sorafenib resistance in patients, organoids and xenograft models²⁴⁸. Independently, insulin-like growth factor 1 receptor (IGF1R)–protein kinase B (AKT)–creatine kinase B (CKB) signalling promotes phosphorylation of serine 104 in GPX4, similarly preventing

CMA-mediated degradation and conferring ferroptosis resistance across HCC, breast, lung and colon cancer models; high levels of threonine 133-phosphorylated and serine 104-phosphorylated GPX4 correlate with reduced levels of the PUFA peroxide 4-hydroxynonenal and unfavourable survival in patients with HCC²⁴⁹.

Additional PTMs reinforce GPX4 stability. Palmitoyltransferase ZDHHC8-mediated S-palmitoylation of GPX4 at cysteine 75 promotes its membrane association in diverse cancer cell lines and patient samples, and drives immune evasion phenotypes in mouse models of melanoma and colorectal cancer²⁵⁰. Additionally, protein arginine N-methyltransferase 5 (PRMT5)-mediated dimethylation of arginine 152 prevents F-box/WD repeat-containing protein 7 (FBW7)–cullin 1 (CUL1)-mediated ubiquitination and thus proteasomal degradation of GPX4, sustaining its expression and limiting ferroptosis in zebrafish and multiple mouse tumour models, including human cell line xenografts²⁵¹.

Metal stress adds a distinct level of regulation. Copper can directly bind to GPX4 at cysteines 107 and 148, inducing its oligomerization, ubiquitination and TAX1-binding protein 1 (TAX1BP1)-dependent macroautophagic degradation⁵. In pancreatic ductal adenocarcinoma xenograft models, oral copper gluconate amplifies IKE-induced ferroptosis, whereas copper chelation preserves GPX4 and mitigates ferroptosis-associated damage⁵.

Finally, the synthetic ferroptosis inducer N6F11 has been shown to bind directly to the E3 ubiquitin/ISG15 ligase TRIM25 and trigger lysine 48 ubiquitination and subsequent proteasomal degradation of GPX4 in cancer cells, thereby enhancing ferroptosis sensitivity and synergizing with anti-PD-L1 antibodies in various xenograft, orthotopic and transgenic tumour models²⁰⁰. By contrast, TRIM59, TRIM46 or TRIM21 promote GPX4 ubiquitination in non-malignant tissues.

Together, these findings underscore GPX4 as a compartmentalized, PTM-governed and metal-responsive enzyme maintained by an integrated network of kinases, acyltransferases, methyltransferases, metal sensors and lipid repair partners.

As a downstream consequence of the coordinated ferroptosis-related processes described above, excessive lipid peroxidation causes catastrophic rupture of plasma membranes, enabling extracellular accumulation and spread of PLOOH that can propagate oxidative injury to neighbouring cells^{72,73}. This plasma membrane rupture can be accelerated by ninjurin 1 (NINJ1)⁷⁴, a pore-forming transmembrane protein originally identified as a key mediator of pyroptosis-associated plasma membrane rupture and damage-associated molecular pattern (DAMP) release⁷⁵, and can also be enhanced by activation of mechanosensitive cation channels, such as Piezo type mechanosensitive ion channel component 1 (PIEZO1)⁷⁶ (Fig. 1). By contrast, ESCRT-III-mediated membrane repair⁷⁷ and/or cadherin 1 (also known as E-cadherin)-dependent activation of the neurofibromin-2–Hippo signalling pathway⁷⁸ can counteract this process, highlighting how tissue architecture, cell density and intercellular adhesion sculpt ferroptotic vulnerability within the tumour microenvironment (TME). Complementing these structural defences, the ALDH superfamily comprises NAD(P)⁺-dependent enzymes that

oxidize reactive aldehydes to their corresponding carboxylic acids; certain members such as ALDH1B1 detoxify lipid-derived aldehydes (for example, 4-hydroxynonenal (4-HNE)) and mitigate oxidative stress, thereby acting as metabolic buffers that limit ferroptosis-associated lipid toxicity⁷⁹ (Fig. 1). Together, these pathways illustrate ferroptosis as a fundamentally membrane-centric form of cell death governed by interconnected metabolic, signalling and organellar networks.

Challenges for clinical translation

Several interdependent barriers – pharmacological, biological, micro-environmental and methodological – continue to impede the translation of ferroptosis from a compelling concept into a viable therapeutic strategy. These challenges are outlined below.

Pharmacological barriers

The clinical translation of ferroptosis-based therapies is hindered by several recurring pharmacological barriers, including poor drug-like

Review article

properties, limited tumour selectivity, suboptimal pharmacokinetics and on-target or off-target toxicities. These limitations manifest differently across distinct classes of ferroptosis inducers but collectively constrain their *in vivo* utility and clinical development (Table 1).

Cystine transport inhibitors such as erastin and its analogues have robust anticancer activity *in vitro*, yet their poor solubility, metabolic instability and limited tumour selectivity preclude meaningful *in vivo* use³. Covalent GPX4 inhibitors, such as RSL3 and ML162, are constrained by their reactive haloacetamide 'warheads', which have broad proteome reactivity, and by suboptimal pharmacokinetics^{24,80}. The nitroisoxazole-based inhibitor ML210 avoids some of this off-target reactivity but is dependent on intracellular metabolic activation (for example, conversion to the α -nitroketoxime JKE-1674) to generate the active electrophile that modifies GPX4, complicating dose–exposure relationships and the predictability of *in vivo* activity⁸¹. Adding to these concerns, recent biochemical analyses using cell-free assays with recombinant GPX4 protein indicate that RSL3 and ML162 do not directly inhibit the enzymatic activity of GPX4, but instead potentially target the selenoenzyme thioredoxin reductase 1 (TXNRD1)⁸². Notably, targeting TXNRD1 using auranofin enhances ferroptosis in

melanoma cell lines and mouse models⁸³. At higher concentrations, RSL3 (and potentially other GPX4 inhibitors) can also elicit mixed cell death programmes, including pyroptosis⁸⁴, raising important questions regarding target specificity and the interpretation of ferroptosis phenotypes observed in cellular systems. Indeed, cytotoxicity induced by high-dose RSL3 is often only partially mitigated by ferroptosis inhibitors, highlighting the involvement of ancillary mechanisms of cell death⁸⁵.

Imidazole ketone erastin (IKE) was designed to improve the metabolic stability and drug-likeness of erastin and has demonstrated ferroptotic anticancer activity in mouse models of lymphoma⁸⁶. Nonetheless, IKE still faces key translational limitations, including poor solubility at physiological pH, a short half-life in both plasma (1.8 h) and tumours (3.5 h), and dose-limiting toxicity of the free-drug formulation, probably owing to systemic inhibition of system xc⁻ and precipitation after injection⁸⁶.

Pharmacological targeting of FSP1 faces similar challenges. Early inhibitors such as iFSP1 have modest potency, incomplete selectivity, unfavourable pharmacokinetics and often preferentially inhibit human over murine FSP1, complicating preclinical validation¹⁵. Newer

Table 1 | Representative ferroptosis inducers and emerging ferroptosis-based therapeutic strategies

Drug class and/or therapeutic strategy	Representative agents	Mechanistic principle	Key limitations	Development stage	Refs.
System xc ⁻ inhibitors	Erastin, IKE	Block cystine import → GSH depletion → GPX4 inactivation	Poor solubility; metabolic instability; systemic cystine-related toxicity	Preclinical (no oncology trials)	2,86
Direct covalent GPX4 inhibitors	RSL3, ML162, ML210, JKE-1674	Covalent GPX4 inhibition → PLOOH accumulation	Highly reactive warheads leading to off-target toxicity; metabolic activation requirement	Preclinical	24,80,81
Allosteric GPX4 modulators	LOC1886	Allosteric destabilization of GPX4	Recent discovery; limited data to date	Early preclinical	198
FSP1 inhibitors	iFSP1, icFSP1, viFSP1, FSEN1	Block FSP1-mediated regeneration of the reduced forms of CoQ ₁₀ (CoQH ₂) and vitamin K (VKH ₂)	Modest potency; FSP1 homologue selectivity (human over murine); unfavourable <i>in vivo</i> pharmacokinetics	Preclinical	15,87–89
Systemic cyst(e)ine depletion	Cyst(e)inase	Extracellular cyst(e)ine degradation → GSH depletion	Risk of general thiol depletion systemically and thus toxicities; immunogenicity; intravenous administration required	Advanced preclinical	27,193
Iron-mobilizing agents	Fentomycin-1, Fe ²⁺ nanoparticles	Expand labile Fe ²⁺ pools → increase Fenton chemistry	Oxidative toxicity; anaemia; local delivery required	Preclinical	64
Lineage-restricted ferroptosis inducers	N6F11	TRIM25-dependent proteasomal degradation of GPX4	TRIM25-restricted activity	Preclinical	200
PROTAC-based degraders	GPX4-PROTAC 8e; FSP1-PROTAC C7	Proteasomal degradation of GPX4 or FSP1	Large molecules; complex pharmacokinetics; E3 ligase-dependence	Preclinical	201,202
Nanotechnology systems	ROS/pH-responsive nanocarriers; hypoxia-activated prodrugs	Tumour-responsive ferroptosis payload release	Manufacturing complexity; biodistribution issues	Preclinical	203
Ferroptosis-payload ADCs	CDH17 × GUCY2C bispecific ADC with RSL3 payload	Targeted delivery of GPX4 inhibitor	Antigen-restricted use; limited ADC stability	Preclinical	205
Clinically used drugs with indirect ferroptotic activity	Sorafenib, gemcitabine, 5-fluorouracil, doxorubicin, statins, sulfasalazine	Indirect ferroptosis induction	Requirement for supraphysiological dosing to induce ferroptosis	Approved (used in combinations with selective ferroptosis inducers preclinically)	199, 240–242

ADC, antibody–drug conjugate; CDH17, cadherin 17; CoQ₁₀, coenzyme Q₁₀; FSP1, ferroptosis suppressor protein 1; GPX4, glutathione peroxidase 4; GSH, glutathione; GUCY2C, guanylyl cyclase C; IKE, imidazole ketone erastin; PLOOH, phospholipid hydroperoxides; PROTAC, proteolysis targeting chimaera; ROS, reactive oxygen species.

agents such as icFSP1 have antitumour activity in mouse xenograft models of melanoma and non-small-cell lung cancer (NSCLC), specifically *GPX4*-knockout models⁸⁷. However, icFSP1 does not directly inhibit the enzymatic activity of FSP1; rather, it induces subcellular relocalization of FSP1 from cell membranes via phase separation, a process in which biomolecules demix to form dynamic, membraneless condensates⁸⁷. By contrast, viFSP1 inhibits both human and murine FSP1 by targeting the highly conserved NAD(P)H-binding pocket of this enzyme⁸⁸. FSEN1 is a highly potent and selective uncompetitive inhibitor of human FSP1 that binds the ternary FSP1–substrate complex and blocks NAD(P)H-dependent CoQ₁₀ regeneration⁸⁹; however, its lack of activity against murine FSP1 continues to pose challenges for preclinical modelling. Furthermore, most studies have used FSP1 inhibition primarily to sensitize cells to *GPX4* loss or *GPX4* inhibitors^{87–89}; although emerging preclinical evidence indicates that FSP1 blockade alone can produce ferroptotic effects against various tumour types in vivo^{90,91}. The therapeutic contexts in which this strategy would be clinically meaningful, either as monotherapy or in combination regimens, remain poorly defined.

Ferroptosis inducers can cause on-target and off-target toxicities. For example, PUFA-rich organs such as the kidney and liver can be sensitized to oxidative injury, while agents that expand the LIP or disrupt ferritin turnover can trigger anaemia, hepatotoxicity or inflammation⁹². Because many ferroptosis inducers also affect broader redox, cytochrome P450 and mitochondrial pathways, toxicity is difficult to predict and often limits dose escalation⁹². These concerns highlight the need for new agents with improved pharmacokinetics, tumour-selective delivery and controllable activation.

Finally, several widely used systemic anticancer therapies (including sorafenib, gemcitabine, 5-fluorouracil and doxorubicin) and natural products (such as withaferin A, curcumin and piperlongumine) can induce ferroptosis (Table 1) – typically in parallel with apoptosis⁹³. Sulfasalazine, an FDA-approved anti-inflammatory drug, has also been explored as a system xc⁻ inhibitor in cell culture and drug repurposing studies in cancer models⁹³. However, the ferroptotic effects of these agents are mechanistically non-specific and generally occur only at stress-inducing concentrations, limiting their value as selective ferroptosis-based therapeutics.

Tumour heterogeneity

Genetic heterogeneity. Genetic diversity is a major determinant of ferroptosis responsiveness. The Kelch-like ECH-associated protein 1 (KEAP1)–NRF2 oxidative stress axis provides a prototypical example. Loss-of-function *KEAP1* mutations result in impaired degradation and thus constitutive activation of NRF2 (Fig. 1). Recurrent alterations in *KEAP1* or NRF2, particularly in NSCLC and HCC, drive persistent upregulation of broad antioxidant programmes and establish a metabolically rewired, ferroptosis-resistant state⁹⁴. In NSCLC, co-mutation of *KEAP1* and *STK11* further reinforces this resistance through SCD1-dependent MUFA synthesis⁹⁵, highlighting the probable importance of mutational profiling for predicting patient response to ferroptosis inducers.

Preclinical studies suggest that certain cancer cells, particularly those in EMT-like states, are exquisitely dependent on *GPX4* and highly sensitive to its inhibition^{10,11,25}. Patient-derived datasets are broadly consistent with the cytoprotective role of *GPX4* in suppressing ferroptosis, with higher *GPX4* expression often being associated with ferroptosis resistance and features of aggressive disease^{96,97}. However, these associations are context-dependent and vary across tumour types, with neutral or favourable correlations with clinical outcomes

reported in certain settings^{91,96}. Collectively, these findings suggest that *GPX4* expression reflects a context-dependent survival advantage but remains insufficiently validated as a predictive biomarker of response to *GPX4*-targeted therapies.

Other genetic alterations exert nuanced, context-dependent effects on sensitivity to ferroptosis. FSP1 is markedly upregulated in ferroptosis-resistant NSCLC and chromophobe renal cell carcinoma (chRCC), and is associated with a poor prognosis^{90,98}, and also promotes tumour growth in mouse models of lung adenocarcinomas, including *KEAP1*-mutant NSCLC⁹⁸. In chRCC, combined inhibition of the SLC7A11–*GPX4* axis and FSP1 yields marked synergy, highlighting the therapeutic potential of concurrently targeting parallel antioxidant pathways⁹⁰.

TP53 mutations can either promote or suppress ferroptosis depending on mutation class, metabolic rewiring and downstream transcriptional programmes. The acetylation-defective p53^{KR} mutant (lysines 117, 161 and 162 substituted with arginine) lacks the canonical cell cycle-related and pro-apoptotic functions of wild-type p53 but retains the non-canonical ability to robustly repress *SLC7A11* expression in human breast cancer and osteosarcoma cell lines, thereby maintaining ferroptotic sensitivity⁹⁹ (Fig. 1). By contrast, *TP53* loss in melanoma and osteosarcoma cell lines derepresses vitamin K epoxide reductase complex subunit 1-like 1 (VKORC1L1), an enzyme that suppresses ferroptosis by generating the reduced, radical-trapping form of vitamin K (VKH₂), thereby attenuating p53-driven ferroptotic programmes¹⁰⁰ (Fig. 1). Conversely, p53 can also inhibit ferroptosis by suppressing dipeptidyl peptidase 4 (DPP4)-dependent activation of NADPH oxidase (NOX) at the plasma membrane, achieved via p53-driven translocation of DPP4 into the nucleus, in human colon cancer cells¹⁰¹ (Fig. 1). Certain p53 mutants exert additional ferroptosis-suppressive functions; for example, p53^{R175H} directly abrogates BACH1-mediated repression of *SLC7A11*, thereby increasing *SLC7A11* expression and promoting tumour growth (Fig. 1) – a mechanism shown in tongue squamous carcinoma cells and validated in cholangiocarcinoma, endometrial carcinoma and *Tp53*^{R172H}-mutant mouse sarcoma models¹⁰².

Early studies suggested a strong link between oncogenic *RAS* mutations and heightened sensitivity to ferroptosis¹⁰³. However, large-scale CRISPR dependency datasets indicate that such mutations do not uniformly confer ferroptosis hypersensitivity¹⁰⁴, suggesting that *RAS*-driven ferroptosis sensitivity is also context-dependent and enriched in specific cancer types, such as PDAC.

Certain tumour-suppressor gene mutations seem to engender more predictable ferroptotic phenotypes. For example, *BRCA1*-deficient tumours, including patient-derived xenografts (PDXs), are vulnerable to combined *GPX4* and poly(ADP-ribose) polymerase (PARP) inhibition, which induces robust ferroptosis in vivo¹⁰⁵. Similarly, orthotopic mouse models of *MYCN*-amplified neuroblastomas demonstrate extreme cysteine dependence and undergo rapid ferroptotic collapse when cysteine metabolism is disrupted¹⁰⁶. Loss-of-function mutations in *BRCA1*-associated protein 1 (BAP1), which normally represses *SLC7A11* expression through epigenetic mechanisms, enhance ferroptosis across multiple cancer cell lines and xenograft models, reinforcing the concept that chromatin-level control of cysteine metabolism is a determinant of ferroptotic liability¹⁰⁷. In addition, activation of or gain-of-function mutations in the PI3K–AKT–mTOR signalling pathway generally increase resistance to ferroptosis across several solid tumour types, via transcriptional upregulation of SCD1 expression and increased *GPX4* protein synthesis^{108–110}, although context-dependent opposing effects have also been reported¹¹¹.

Epigenetic heterogeneity. Epigenetic programmes add an additional axis of heterogeneity beyond genotype. DNA methylation regulates the expression of core ferroptosis genes such as *SLC7A11* (ref. 112) and *ACSL4* (ref. 113), thus reshaping GSH synthesis and PUFA-PL generation. Histone modifiers, including bromodomain-containing protein 4 (BRD4)¹¹⁴ and lysine-specific demethylase 3B (KDM3B)¹¹⁵, directly regulate GPX4-dependent and SLC7A11-dependent transcriptional programmes. Non-coding RNAs such as miR-137 (ref. 116) further tune redox and lipid peroxidation pathways. Therapy-induced chromatin remodelling adds further plasticity: in melanoma with secondary resistance to BRAF and MEK inhibitors, dynamic focal amplifications of *BRAF*^{V600E} (intrachromosomal or extrachromosomal), as well as in other MAPK pathway genes such as *RAF1* and *NRAS*, promote oxidative phosphorylation (OXPHOS), GSH depletion and NCOA4-dependent ferritinophagy, creating an acquired GPX4 inhibitor-sensitive state that is independent of dedifferentiation¹¹⁷.

Metabolic heterogeneity. Metabolic diversity introduces further layers of variation. Spatially resolved multiomic analyses of human ccRCC²⁵ and melanoma¹¹⁸ tumours have revealed discrete metabolic niches enriched in PUFA-PLs generated either by ACSL4–LPCAT3-dependent synthesis or via endothelial-driven remodelling of lipid metabolism mediated by hypoxia-inducible factor 2 α (HIF2 α ; also known as EPAS1) and hypoxia-inducible lipid droplet-associated protein (HILPDA). These regions demonstrate pronounced GPX4 dependence and heightened vulnerability to ferroptosis, illustrating how local nutrient and oxygen gradients can sculpt ferroptotic sensitivity across tumour ecosystems^{25,118}. Conversely, tumours with elevated expression of ACSL3 or SCD1 accumulate MUFAs and resist ferroptosis, frequently overlapping with radiotherapy-tolerant microdomains^{51,52,119}. Spatial variation in iron handling, including TFRC levels¹²⁰, NCOA4-dependent ferritinophagy³⁹ and HIF2 α -regulated expression of iron-related genes¹²¹, is likely to further modulate local LIPs and lipid peroxidation thresholds.

Additional metabolic pathways shape tumour-specific ferroptosis phenotypes. In mouse models of ccRCC, glycosaminoglycan-dependent lipoprotein uptake enhances ferroptosis resistance, and loss of glycosaminoglycan biosynthesis sensitizes tumours to ferroptosis¹²². These findings highlight how extracellular matrix-derived metabolic inputs can unexpectedly modulate ferroptotic vulnerability. Mitochondria-linked nucleotide metabolism provides another layer of protection. The ‘pyrimidinosome’ – a multi-enzyme assembly physically coupled to mitochondrial DHODH – coordinates pyrimidine production with DHODH-mediated detoxification of lipid peroxides¹²³. This coupling creates a selective vulnerability in AMPK-low tumours, which rely disproportionately on DHODH for redox maintenance and, therefore, demonstrate heightened sensitivity to combined nucleotide and antioxidant pathway inhibition¹²³. High-OXPHOS high-grade serous ovarian cancer offers a contrasting paradigm: chronic oxidative stress and promyelocytic leukaemia protein (PML)–peroxisome proliferator-activated receptor- γ (PPARG) coactivator 1 α (PPARGC1 α)-driven mitochondrial biogenesis amplifies ROS production and simultaneously elevates ferroptotic susceptibility, rendering these tumours more responsive to chemotherapy¹²⁴. In PDAC and other ferroptosis-prone malignancies, the E3 ubiquitin protein ligase Praja 1 induces degradation of lactoylglutathione lyase (also known as methylglyoxalase), thereby triggering methylglyoxal accumulation that leads to autophagic degradation of ferritin and GPX4 (ref. 125). This metabolic cascade expands the LIP while disabling the core lipid peroxide

detoxification machinery, thus forming a potent feedforward circuit that amplifies ferroptosis vulnerability¹²⁵.

Certain metabolites also exert striking context-dependent effects on ferroptosis. 7-Dehydrocholesterol (7-DHC) is generated by lathosterol oxidase as the penultimate step of the distal cholesterol biosynthesis pathway (Fig. 1); the terminal step is then catalysed by 7-DHC reductase (DHCR7), which reduces 7-DHC to cholesterol. Pharmacological or genetic inhibition of DHCR7 causes an accumulation of 7-DHC, a sterol with exceptionally high RTA potency that can suppress ferroptosis^{126,127}. Under heightened oxidative stress, however, accumulated 7-DHC is rapidly oxidized by ROS into cytotoxic oxysterols such as 25-hydroxycholesterol (25-OHC), which instead exacerbate lipid peroxidation and ferroptotic damage¹²⁸. The immunometabolite itaconate, generated by *cis*-aconitate decarboxylase 1, is strongly upregulated in inflammatory macrophages and exerts dual immunomodulatory effects by alkylating cysteine residues on target proteins¹²⁹. Similarly, itaconate can suppress ferroptosis through NRF2 activation in melanoma and colon cancer cells¹³⁰ or promote neutrophil survival in models of breast cancer via granulocyte–macrophage colony-stimulating factor (GM-CSF)–signal transducer and activator of transcription 5 (STAT5)–CCAAT/enhancer-binding protein- β (CEBPB) signalling¹³¹. By contrast, in drug-tolerant retinoblastoma cells, itaconate enhances ferritinophagy and thereby promotes ferroptosis¹³². In addition, emerging evidence suggests that polyamines can chelate labile Fe²⁺ and buffer lipid peroxidation, thereby conferring ferroptosis resistance in leukaemia¹³³.

Lineage-driven heterogeneity. Lineage identity and dynamic cell-state transitions provide further heterogeneity in susceptibility to ferroptosis. In contrast to non-malignant melanocytes, which possess strong antioxidant defences, undifferentiated melanoma cells are intrinsically ferroptosis-prone owing to low melanocyte-inducing transcription factor (MITF) and high AXL receptor tyrosine kinase activity¹³⁴. Therapy-induced dedifferentiation – for example, as an acquired mechanism of BRAF–MEK inhibitor resistance or following cytokine exposure – drives melanoma cells towards these vulnerable states, highlighting ferroptosis as a dynamic, plastic liability¹³⁴. Autophagy status also varies across cancer cells: some require ferritinophagy-derived iron^{39,40} or lipophagy-derived lipids⁷¹ for the initiation of lipid peroxidation, implying that cells with resistance to these autophagy-dependent mechanisms are likely to survive⁴³. Defining the selective autophagy pathways that mediate ferroptosis in each cellular state will be crucial for overcoming this heterogeneity.

Lineage-specific metabolic programming further influences ferroptosis thresholds. Cancer cells at invasive tumour fronts and/or metastatic sites often show upregulation of SLC7A11 expression to buffer lipid peroxidation¹³⁵. By contrast, mesenchymal or EMT-like states, including PHF8-mediated or zinc finger E-box-binding homeobox 1 (ZEB1)-driven programmes, are associated with heightened sensitivity to GPX4 inhibition owing to coordinated upregulation of PUFA synthesis enzymes (for example, ACSL4) and concomitant downregulation of MUFA synthesis pathways (including SCD1)^{41,136,137} (Fig. 1). In patients with TNBC, an integrated multiomic analysis identified ferroptosis-high and ferroptosis-low molecular subgroups; ferroptosis-high tumours have elevated ACSL4 and PUFA-PL signatures and in mouse models respond more favourably to ferroptosis inducers (such as GPX4 inhibitors) combined with immunotherapies (such as anti-PD-1 antibodies) than their ferroptosis-low counterparts¹³⁸. In patients with HCC, ACSL4 expression predicts responsiveness to

sorafenib, reflecting variability in ferroptosis sensitivity¹³⁹. However, how ACSL4 expression is gained, maintained or lost across tumour lineages, and how this regulation shifts during progression, therapy and metastasis, remain important unanswered questions.

Biological sex-related heterogeneity. Sex differences introduce yet another layer of heterogeneity. Preclinical evidence indicates that sex hormones suppress ferroptosis in oestrogen receptor-positive breast and androgen receptor-positive prostate cancers via membrane-bound glycerophospholipid *O*-acyltransferase 1 and/or 2 (MBOAT1/2)-mediated phospholipid remodelling to produce PUFAs, establishing a GPX4-independent and FSP1-independent protective axis¹⁴⁰ (Fig. 1). In colorectal cancer (CRC), only *KRAS*-mutant tumours from male patients have reduced ferroptosis potential and are associated with inferior outcomes compared with *KRAS*-wild-type tumours, illustrating context-specific sex–genotype interactions¹⁴¹. Pan-cancer analyses have further revealed broad sex-dependent variation in ferroptosis signatures, immune infiltration and prognostic associations¹⁴².

Together, these genetic, epigenetic, metabolic, lineage-dependent and sex-related factors shape a highly heterogeneous and dynamic ferroptosis landscape within individual tumours. This diversity underlies the wide variability in sensitivity to ferroptosis observed across experimental models and patient-derived samples, and helps to explain why single-agent ferroptosis inducers rarely yield durable therapeutic benefit. From a clinical perspective, these findings argue against uniform ferroptosis-targeted strategies and instead support biomarker-guided patient stratification, rational combination therapies and spatially informed treatment approaches that account for intratumoural metabolic and lineage heterogeneity. Defining context-specific ferroptotic liabilities will, therefore, be essential for translating ferroptosis-based interventions into effective and durable cancer therapies.

Tumour microenvironment

The stromal TME imposes fundamental metabolic constraints, most notably hypoxia and acidosis, that shape ferroptosis sensitivity at a systems level. By modulating iron availability, lipid composition, redox balance and immune signalling, these TME features generate spatially heterogeneous niches in which ferroptosis can be either promoted or restrained.

Stromal populations, including cancer-associated fibroblasts (CAFs) and other metabolically active cells in the TME, can buffer ferroptotic stress. In PDAC models, cancer cells secrete transforming growth factor- β (TGF β), which acts on CAFs via TGF β receptor type 1 (TGF β R1)¹⁴³. TGF β R1 signalling activates a SMAD family member 3 (SMAD3)–ATF4 transcriptional programme, thereby upregulating cysteine biosynthetic and cysteine export pathways in CAFs¹⁴³. The exported cysteine can then be taken up by cancer cells via solute carrier family 1 members 1, 4 and/or 5 (SLC1A1/4/5) transporters to support GSH synthesis and suppress ferroptosis¹⁴³ (Fig. 3a). Indeed, genetic or pharmacological inhibition of stromal cysteine biosynthesis – achieved by targeting cystathionine- β synthase (CBS) in CAFs – restores cancer cell sensitivity to ferroptosis in mouse xenograft models of PDAC¹⁴³. Extracellular antioxidants and stromal-derived lipids further reinforce ferroptosis-resistant niches^{144,145}, highlighting that ferroptosis induction is not purely cancer cell-autonomous.

Hypoxia – prevalent in most solid tumours – rewires lipid and iron metabolism in a manner that suppresses ferroptosis. Activation of HIF1 α enhances glutamate uptake via transcriptional upregulation of SLC1A1 (ref. 146), might promote fatty acid-binding protein 3

(FABP3)-dependent lipid droplet accumulation in prostate cancer cells via downregulation of genes including *ACSL4* and *LPCAT3* (ref. 147), and also promotes cystine uptake in HCC cells by stabilizing SLC7A11 expression (at the mRNA level via transcriptional suppression of the *N*⁶-adenosine-methyltransferase *METTL14*)¹⁴⁸ (Fig. 3b). Obesity-linked signalling intersects with hypoxic signalling. For example, loss-of-function *VHL* alterations in ccRCC cells result in HIF2 α -dependent expression of the adipokine retinoic acid receptor responder proteins 2 (RARRES2; also known as chemerin), which suppresses fatty acid oxidation and thus lipid ROS levels, thereby conferring resistance to ferroptosis¹⁴⁹ (Fig. 3b). Conversely, in *VHL*-deficient ccRCC, HIF2 α can drive a lipid-rich metabolic state that increases sensitivity to ferroptosis¹⁵⁰, highlighting how hypoxia might create either protective or vulnerable states depending on genetic context. Non-canonical hypoxia responses also contribute: suppression of KDM6A under prolonged hypoxia results in transcriptional repression of *ACSL4* and ethanolamine kinase 1 (ETNK1), shifting phospholipid metabolism towards ferroptosis resistance in ccRCC cells¹⁵¹ (Fig. 3b). In oesophageal squamous cell carcinoma cells, hypoxia-mediated downregulation of the protein deubiquitinating enzyme ubiquitin-specific processing protease 2 (USP2) impairs NCOA4 stability, ferritinophagy and ferroptosis¹⁵². In sharp contrast, high-oxygen environments such as the lung impose selective pressure for NFS1 cysteine desulfurase activity; *NFS1* loss destabilizes Fe–S clusters, activates the iron starvation response and synergizes with cystine import inhibition to trigger ferroptosis in lung cancer models¹⁵³. Together, these findings illustrate how oxygen tension – and its intersection with oncogenic and metabolic programmes – acts as a powerful regulator of vulnerability to ferroptosis.

Tumour acidosis, driven by glycolysis and lactate accumulation, exerts context-dependent effects. Acidic pH enhances uptake and peroxidation of ω 3 and ω 6 PUFAs and can sensitize cancer cells to ferroptosis when antioxidant capacity is exceeded in models of fibrosarcoma and ccRCC¹⁵⁴. Conversely, HIF1 α -driven lactate production by lactate dehydrogenase (LDH), together with broader glycolytic rewiring, protects cancer cells from lipid peroxidation across various solid tumour types^{146,155} (Fig. 3b). Given that acidity also alters stromal and immune cell function, acidosis might generate focal ferroptosis-prone zones while protecting adjacent cell populations. Otherwise, chronic acidosis can reinforce metabolic programmes such as lactate-driven NAD⁺ regeneration, monocarboxylate transporter-mediated redox coupling and HIF1 α -stabilizing feedback loops that collectively suppress ferroptosis and sustain therapy-resistant niches.

Ferroptosis engages the immune TME in complex, bidirectional ways. Ferroptotic tumour cells release DAMPs such as ATP, decorin and high mobility group box 1 (HMGB1), as well as oxidized phospholipids and other inflammatory mediators that activate dendritic cells (DCs) and support antitumour immunity^{156–158} (Fig. 3c). Conversely, immunosuppressive factors, including prostaglandin E₂ (PGE₂) produced in the TME or released by ferroptotic cancer cells, can blunt IL-2 sensing in CD8⁺ tumour-infiltrating lymphocytes^{159,160} (Fig. 3c). Data published in 2026 further reveal that GPX4, selectively released during ferroptosis, binds zona pellucida glycoprotein 3 (ZP3) on conventional type 1 DCs (cDC1), triggering cAMP–protein kinase A (PKA)–6-phosphofructo-2-kinase/fructose-2,6-biphosphatase 2 (PFKFB2) signalling to suppress glycolysis, antigen presentation and CD8⁺ T cell priming¹⁶⁰. This GPX4–ZP3 checkpoint functions across KPC transgenic, orthotopic and syngeneic PDAC models, thereby dampening responses to chemotherapy, radiotherapy and immune checkpoint inhibitors (ICIs)¹⁶⁰

Review article

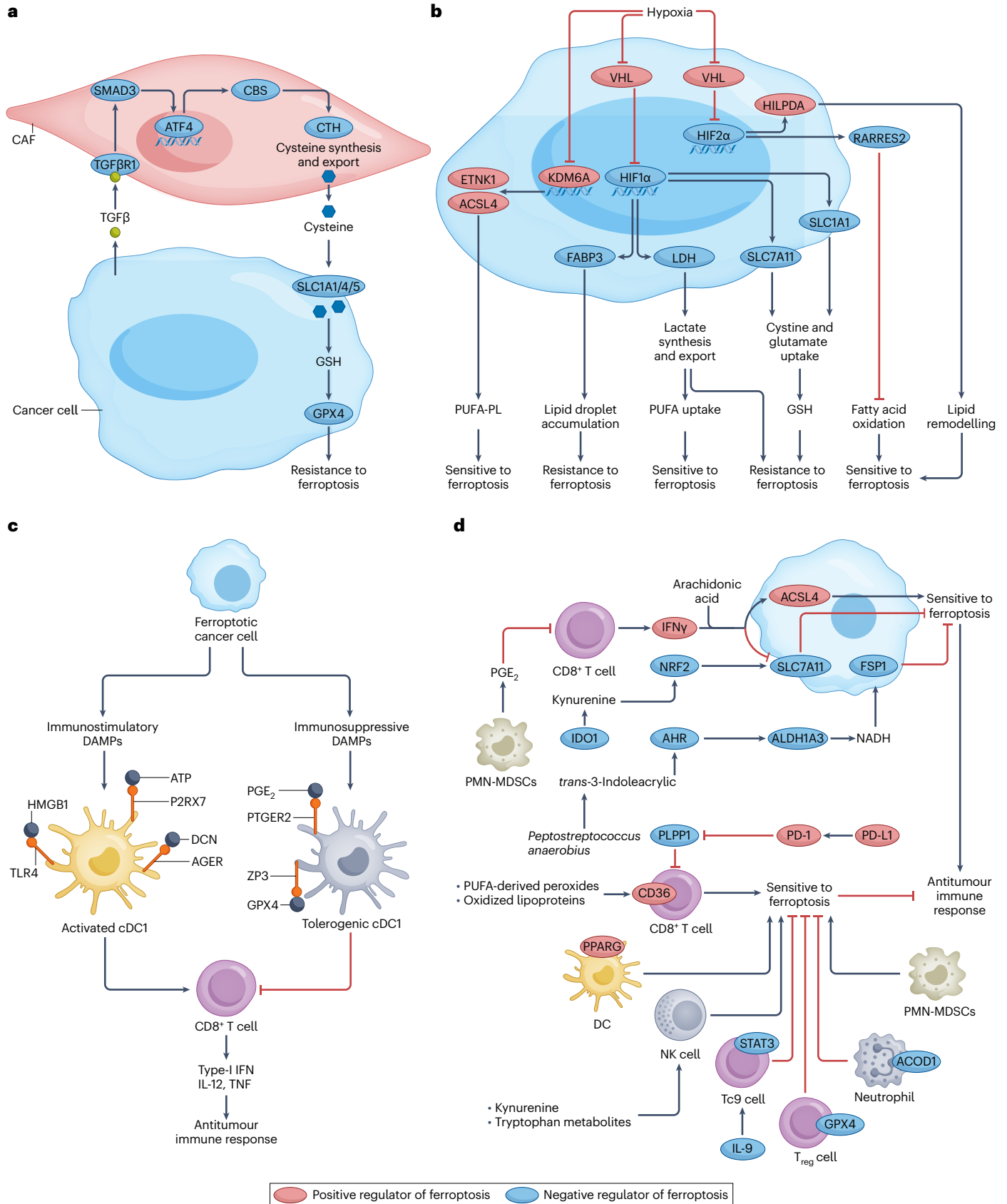


Fig. 3 | Microenvironmental and immune determinants of ferroptosis sensitivity in cancer. **a**, Cancer-associated fibroblasts (CAF) can promote cancer cell resistance to ferroptosis via a transforming growth factor- β (TGF β)-induced signalling axis, which upregulates expression of cystathionine β -synthase (CBS) and cystathionine γ -lyase (CTH), thereby enhancing cysteine synthesis and export. Cancer cells can import cysteine via solute carrier family 1 members 1, 4 and/or 5 (SLC1A1/4/5) to sustain glutathione (GSH) synthesis and thus the antioxidant activity of GSH peroxidase 4 (GPX4), thereby providing protection from ferroptotic lipid peroxidation. **b**, Hypoxia suppresses von Hippel–Lindau protein (VHL)-mediated proteasomal degradation of hypoxia-inducible factor 1 α (HIF1 α) and HIF2 α , thus enabling these transcription factors to drive metabolic programmes that bidirectionally influence ferroptosis. HIF1 α /2 α -dependent lactate production, polyunsaturated fatty acid (PUFA) uptake, lipid droplet accumulation and/or hypoxia-inducible lipid droplet-associated protein (HILPDA)-mediated lipid remodelling enhance ferroptosis sensitivity. By contrast, HIF1 α -induced upregulation of SLC7A11 and SLC1A1 expression enhances cystine and glutamate uptake to promote resistance to ferroptosis, and HIF2 α -dependent expression of retinoic acid receptor responder protein 2 (RARRES2) suppresses fatty acid oxidation and thus ferroptosis. In addition, hypoxia suppresses the oxygen-dependent activity of lysine-specific histone demethylase 6A (KDM6A), thereby reducing expression of its lipid metabolism-related target genes (including *ACSL4* and *ETNK1*) and thus rewiring phospholipid composition towards a ferroptosis-resistant state. **c**, Ferroptotic cancer cells release both immunostimulatory and immunosuppressive damage-associated molecular patterns (DAMPs). For example, extracellular high mobility group box 1 (HMGB1), ATP and decorin

(DCN) activate conventional type 1 dendritic cells (cDC1) to prime CD8⁺ T cells, whereas GPX4 and prostaglandin E₂ (PGE₂) drive tolerogenic dendritic cell (DC) states and dampen antitumour immunity. **d**, Immune cell-intrinsic lipid metabolism also influences ferroptosis sensitivity. Long-chain fatty acid CoA ligase 4 (ACSL4) promotes PUFA phospholipid (PUFA-PL) peroxidation and thus ferroptosis in cancer cells, whereas SLC7A11, ferroptosis suppressor protein 1 (FSP1) and aldehyde dehydrogenase 1 family member A3 (ALDH1A3; also known as retinaldehyde dehydrogenase 3) provide antioxidant protection. In addition, interferon (IFN)- γ (IFN γ) released by CD8⁺ T cells increases cancer cell sensitivity to ferroptosis by upregulating ACSL4 expression and downregulating SLC7A11 expression. PD-L1–PD-1 signalling enhances the sensitivity of CD8⁺ T cells to ferroptosis by downregulating phospholipid phosphatase 1 (PLPP1). In addition, microbial metabolites that activate aryl hydrocarbon receptor (AHR) signalling, CD36-mediated uptake of oxidized lipid, signal transducer and activator of transcription 3 (STAT3)-dependent IL-9-producing CD8⁺ cytotoxic T (Tc9) cells, peroxisome proliferator-activated receptor- γ (PPARG)-regulated DCs, aconitate decarboxylase 1 (ACOD1)-expressing neutrophils, polymorphonuclear myeloid-derived suppressor cells (PMN-MDSCs), natural killer (NK) cells and regulatory T (T_{reg}) cells all collectively integrate ferroptotic stress to shape antitumour immunity. AGER, advanced glycosylation end product-specific receptor; ATF4, cAMP-dependent transcription factor ATF4; ETNK1, ethanolamine kinase 1; FABP3, fatty acid-binding protein 3; IDO1, indoleamine 2,3-dioxygenase 1; LDH, lactate dehydrogenase; NRF2, nuclear factor erythroid 2-related factor 2; P2RX7, P2X purinoceptor 7; PTGER2, prostaglandin E₂ receptor EP2 subtype; SMAD3, SMAD family member 3; TGF β RI, TGF β receptor 1; TLR4, Toll-like receptor 4; TNF, tumour necrosis factor; ZP3, zona pellucida sperm-binding protein 3.

(Fig. 3c). In parallel, excessive lipid peroxidation within immune cells in the TME can impair antigen processing, cytokine production and effector differentiation^{161,162}. By contrast, CD8⁺ T cell-derived interferon- γ (IFN γ) increases the sensitivity of cancer cells to ferroptosis via downregulation of SLC7A11 and upregulation of ACSL4, and this effect is further potentiated by arachidonic acid, which is often present in the TME^{163,164} (Fig. 3d). Together, these opposing pathways underscore the need to carefully calibrate ferroptosis induction to avoid immune dysfunction while preserving therapeutic responsiveness, particularly during immunotherapy.

The tumour-associated microbiota is increasingly recognized as a regulator of ferroptosis. In models of CRC, the indole metabolite *trans*-3-indoleacrylic acid, produced by *Peptostreptococcus anaerobius*, activates the AHR–ALDH1A3–FSP1–CoQ₁₀ axis, thereby suppressing lipid peroxidation and creating a ferroptosis-resistant niche that accelerates tumour growth¹⁶⁵ (Fig. 3d). Host indoleamine 2,3-dioxygenase 1 (IDO1)-dependent kynurenine metabolism similarly generates anti-ferroptotic signals via NRF2-dependent SLC7A11 expression as well as through direct ROS scavenging by downstream kynurenine metabolites, as demonstrated across multiple solid tumour cell line models¹⁶⁶ (Fig. 3d). Although direct evidence that intratumoural bacteria trigger or block ferroptosis in cancer cells remains limited¹⁶⁷, infection models demonstrate that bacterial quorum-sensing molecules can induce ferroptosis-like death in myeloid cells, suggesting mechanistic parallels¹⁶⁸. Yet, whether microbial communities actively sculpt a ferroptosis-resistant TME or simply adapt to pre-existing redox conditions remains unresolved, and dissecting these causal interactions will require spatial, metabolomic and gnotobiotic approaches.

Together, these TME-dependent processes demonstrate that ferroptosis induction is inherently spatially restricted and thus pharmacological ferroptosis inducers are unlikely to be uniformly effective without TME-informed strategies. Overcoming stromal buffering,

hypoxia, acidosis, immune vulnerability and microbiota-derived mediators of resistance, rather than targeting of cancer cells alone, will be essential for successful clinical translation of ferroptosis-targeted therapies.

Differential influence across the disease course

Ferroptosis is not a uniform cell death end point but a dynamic process that influences tumour initiation, clonal evolution and metastatic adaptation in a manner dependent on the stage of tumorigenesis (Fig. 4). Data suggest that ferroptosis can promote tumour initiation via various mechanisms. In genetically engineered mouse models of oncogenic *Kras*-driven PDAC, a high-iron diet or pancreas-specific *Gpx4* deletion triggers the release of oxidized nucleobases such as 8-hydroxyguanosine (8-OHG), which activate the stimulator of interferon genes protein (STING)-dependent DNA-sensing pathway, thereby promoting macrophage recruitment, acinar–ductal metaplasia and tumour initiation¹⁶⁹. Once PDAC is established, however, cancer cells acquire a marked dependence on system xc⁻-mediated cystine import and GPX4 to suppress lipid ROS toxicity; genetic ablation of *Slc7a11* in autochthonous models of PDAC leads to catastrophic ferroptosis, tumour collapse and prolonged survival²⁷, underscoring ferroptosis as a potent intrinsic tumour-suppressive pressure during tumour progression.

Ferroptosis also influences metastatic organotropism. In mouse models of PDAC, proprotein convertase subtilisin–kexin type 9 (PCSK9)-high cancer cells preferentially colonize the oxygen-rich lung by activating distal cholesterol biosynthetic pathways that generate 7-DHC derivatives to suppress ferroptosis¹⁷⁰ (Fig. 4). By contrast, PCSK9-low cells seed the LDL-rich liver, where exogenous cholesterol supports mTORC1-driven niche adaptation¹⁷⁰. Modulating PCSK9 alone can redirect metastatic tropism¹⁷⁰, underscoring how distinct oxidative environments select for subclones with specific ferroptotic liabilities. Consistent with the findings in PDAC models, tumour-restricted loss of

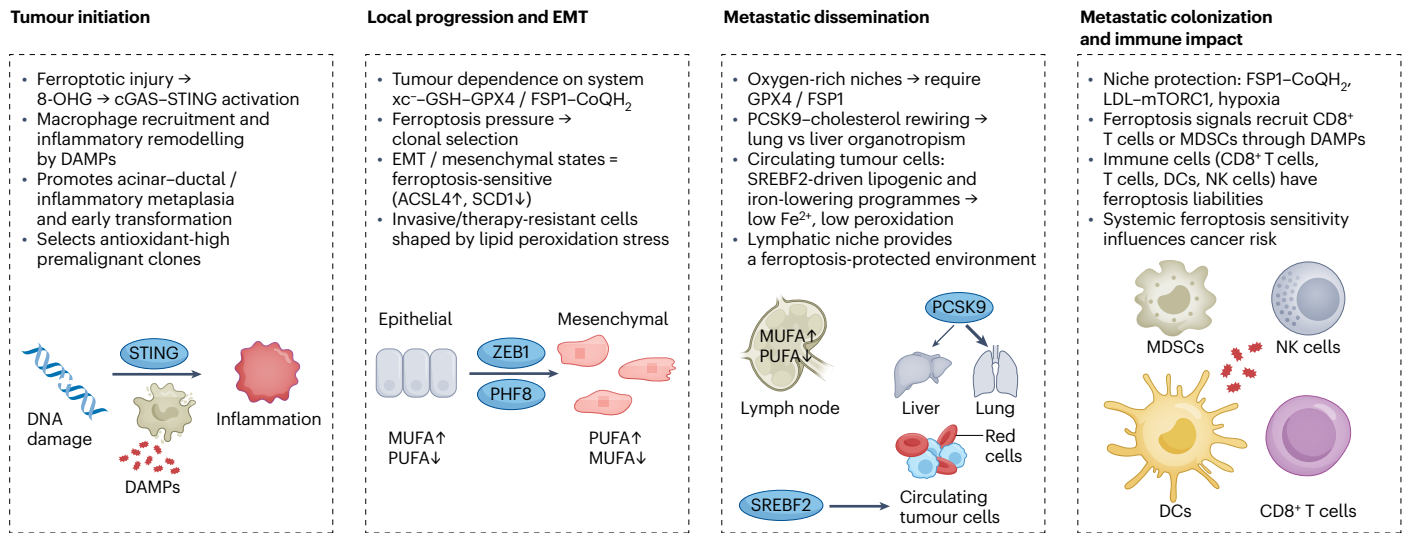


Fig. 4 | Stage-specific roles of ferroptosis throughout tumour evolution. Ferroptosis shapes tumour development and progression through distinct, stage-dependent mechanisms. During tumour initiation, ferroptotic stress can be tumour-promoting by driving inflammatory remodelling and selecting for premalignant cell populations with enhanced antioxidant capacity. During local tumour progression and epithelial–mesenchymal transition (EMT), ferroptosis acts predominantly as a tumour-suppressive pressure, enforcing dependence on antioxidant defence mechanisms and shaping invasive and therapy-resistant lineages. During metastatic dissemination, ferroptosis imposes a selective constraint on circulating and disseminated tumour cells, such that survival in distinct organ niches requires effective ferroptosis resistance. In established metastatic lesions, ferroptosis resistance supports tumour persistence and contributes to immunosuppression, whereas ferroptotic

cues can exert dual effects by recruiting immune cells while simultaneously compromising ferroptosis-sensitive antitumour immune populations. 8-OHG, 8-hydroxyguanosine; ACSL4, long-chain fatty acid CoA ligase 4; cGAS, cyclic GMP–AMP synthase; CoQH₂, reduced coenzyme Q₁₀ (ubiquinol); DAMPs, damage-associated molecular patterns; DCs, dendritic cells; FSP1, ferroptosis suppressor protein 1; GPX4, glutathione peroxidase 4; GSH, glutathione; MDSCs, myeloid-derived suppressor cells; mTORC1, mechanistic target of rapamycin complex 1; MUFA, monounsaturated fatty acid; NK, natural killer; PCSK9, proprotein convertase subtilisin–kexin type 9; PUFA, polyunsaturated fatty acid; SCD1, stearoyl CoA desaturase; SREBF2, sterol regulatory element-binding transcription factor 2; STING, stimulator of interferon gene protein; system xc⁻, cystine–glutamate antiporter system; ZEB1, zinc finger E-box-binding homeobox 1.

Gpx4 or *Aifm2* (encoding FSP1) in models of *Kras*-driven lung adenocarcinoma markedly impairs early tumour outgrowth⁹¹, highlighting the essential role of GPX4 and FSP1 in oxygen-rich metastatic niches (Fig. 4).

In mouse models of hepatocarcinogenesis, ferroptotic signalling intersects with innate immunity to influence tumour initiation and immune composition. Hepatocyte-specific *Gpx4* loss triggers ferroptotic injury that generates oxidative DNA adducts, activates cyclic GMP–AMP synthase (cGAS)–STING signalling, recruits CD8⁺ T cells in a CXC motif chemokine ligand 10 (CXCL10)-dependent manner and induces IFN γ -driven expression of PD-L1, while ferroptosis-derived HMGB1 promotes myeloid-derived suppressor cell (MDSC) infiltration¹⁷¹ (Fig. 4). Liver *Atf4* deficiency also heightens ferroptotic susceptibility via *Slc7a11* repression, leading to exaggerated lipid peroxidation, necroinflammation and accelerated diethylnitrosamine-induced tumour formation¹⁷². Moreover, pericentral hepatocytes exhibit intrinsic ferroptosis resistance owing to high levels of GST- μ 2 and GST- μ 3 expression, enabling them to endure oxidative stress and serve as dominant cells of origin for HCC¹⁷³.

Resistance to ferroptosis also enhances metastatic fitness. In mouse models of melanoma, circulating tumour cells face extreme oxidative stress and remain acutely GPX4-dependent¹⁷⁴, whereas lymph node metastases adapt to hypoxia by upregulating FSP1-mediated CoQ₁₀ regeneration, which confers ferroptosis resistance³². These observations suggest that the lymphatic niche provides a ferroptosis-protected environment that supports metastatic cell

survival and dissemination. Circulating melanoma cells can further activate sterol regulatory element-binding transcription factor 2 (SREBF2)-driven lipogenic and iron homeostatic programmes, including transcriptional upregulation of transferrin, to lower labile iron levels and limit lipid peroxidation, thereby enhancing metastatic seeding¹⁷⁵ (Fig. 4). In models of ovarian cancer, metastatic cells acquire an ACSL4-driven PUFA-enriched membrane state that promotes extravasation but simultaneously heightens ferroptosis sensitivity, exposing a therapeutically exploitable metabolic vulnerability¹⁷⁶. Ferroptosis also influences systemic cancer susceptibility, with excessive ferroptotic loss of CD8⁺ T cells linked to increased cancer risk in individuals with sickle cell disease¹⁷⁷.

Although EMT does not initiate tumorigenesis, partial EMT states can facilitate early tumour progression by enhancing cancer cell survival, stemness, invasiveness and metabolism once oncogenic transformation has occurred. As noted earlier in this Review, cancer cells with an EMT-like phenotype have heightened sensitivity to GPX4 inhibition owing to PUFA-enriched membranes (Fig. 4), supporting the rationale for ferroptosis-based strategies in advanced-stage tumours^{10,11}. However, because many antitumour immune cells are themselves highly sensitive to ferroptosis (as discussed further in the following subsection), non-selective or systemic ferroptosis induction risks dampening overall antitumour immunity.

Together, these observations position ferroptosis as a bidirectional determinant of cancer evolution, which is capable of promoting

inflammatory transformation of neoplastic cells at early stages of tumour development while constraining tumour growth and metastatic colonization once ferroptotic pressure exceeds cellular antioxidant capacity. Notably, evidence linking ferroptotic damage to tumorigenesis has largely been derived from conditional *Gpx4* deletion models, which might incompletely reflect physiological tumour initiation in humans. From a translational perspective, these findings support ferroptosis induction as a potentially effective anticancer strategy but also underscore the need for careful therapeutic calibration, given the risk that sublethal or spatially restricted ferroptotic stress could foster tumour-promoting inflammation and/or secondary malignancies. Moreover, distinct ferroptosis-buffering systems, such as GPX4-dependent versus FSPI-mediated protection, might need to be selectively targeted depending on tumour context, metastatic niche and microenvironmental constraints.

Adverse effects

A key challenge for clinical translation of ferroptosis inducers relates to the ferroptosis sensitivity of antitumour immune cells (Fig. 3d). Targeted lipidomics has revealed that non-malignant T cells and B cells have exceptionally high levels of PUFA-PLs, and these cells are intrinsically more ferroptosis-prone than monocytes or neutrophils – the latter becoming susceptible only when levels of PUFA-PL and NOX2-derived ROS rise¹⁷⁸. Cytotoxic CD8⁺ T cells, particularly CD36⁺-exhausted subsets, readily accumulate PUFA-derived peroxides and oxidized lipoproteins in lipid-rich TMEs, as shown across melanoma, CRC and HCC models^{161,179}. This lipid stress suppresses GPX4, activates p38 signalling and drives functional exhaustion or ferroptotic death^{161,179}. Restoring GPX4 expression or blocking CD36-mediated PUFA uptake, thereby reducing lipid-driven oxidative stress and preserving T cell effector function, and thus a humanized anti-CD36 antibody (PLT012) enhances the antitumour activity of ICIs in models of HCC¹⁸⁰. In addition, PD-1 signalling induces erythroid transcription factor (also known as GATA1)-dependent repression of phospholipid phosphatase 1 (PLPP1), leading to impaired phosphatidylcholine and phosphatidylethanolamine synthesis and depletion of PUFA-PLs¹⁸¹. This disruption of phospholipid homeostasis compromises membrane integrity and lipid-buffering capacity, thereby sensitizing CD8⁺ T cells to lipid-driven ferroptosis in the presence of unsaturated fatty acids in the TME (Fig. 3d), as shown in models of melanoma, lung and oesophageal cancers; in these models, PD-1 blockade rescues T cell function only when PLPP1 is intact¹⁸¹. These findings emphasize that non-selective induction of ferroptosis might inadvertently undermine immunotherapy.

Other immune cell subsets show distinct ferroptosis dependencies. IL-9-producing CD8⁺ effector T (Tc9) cells are relatively resistant to ferroptosis, reflecting IL-9–STAT3 signalling and associated fatty acid oxidation programmes that limit lipid peroxidation¹⁸² (Fig. 3d). Moreover, regulatory T (T_{reg}) cells are highly dependent on GPX4 to suppress lipid peroxidation and ferroptosis; genetic or pharmacological disruption of GPX4 renders T_{reg} cells ferroptosis-prone, leading to mitochondrial superoxide accumulation, IL-1 β production and secondary activation of T helper 17 (T_H17) cell responses¹⁸³. DCs rapidly lose antigen-presenting capacity following GPX4 inhibition through PPAR γ -mediated metabolic rewiring¹⁶². Tumour-associated natural killer (NK) cells likewise become highly ferroptosis-prone in the presence of L-kynurenine and other tryptophan metabolites (Fig. 3d), and NK cells isolated from human ovarian cancer ascites, OVCAR8 xenografts or gastric and lung tumours have pronounced levels of lipid peroxidation, mitochondrial dysfunction and ferroptosis-like

injury^{184,185}. These findings identify ferroptotic injury as a new driver of NK cell dysfunction in solid tumours and demonstrate that NRF2 activation (for example, with RTA-408) can restore NK cell metabolism and antitumour activity^{184,185}. Myeloid cells add further complexity. Polymorphonuclear MDSCs undergoing ferroptosis release oxygenated lipids and PGE₂ that dampen T cell-mediated cytotoxicity (Fig. 3d); therefore, inhibiting ferroptosis in MDSCs improves ICI responses in preclinical models¹⁸⁶. By contrast, conditional *Gpx4* deletion to selectively promote ferroptosis in T_{reg} cells enhances antitumour immunity and improves cancer control in transgenic mouse models¹⁸³. These bidirectional consequences illustrate the need to preserve immune fitness while targeting tumour-intrinsic ferroptosis.

Haematopoietic toxicity is an additional liability of ferroptosis inducers. Human haematopoietic stem cells operate at low basal antioxidant capacity and are, therefore, vulnerable to GPX4 inhibition or cystine deprivation^{187,188}. Certain organs with high oxidative throughput, particularly the liver and kidney, are also intrinsically susceptible owing to a high dependence on ferroptotic regulators including GPX4 (refs. 14,189); in mice, conditional *Gpx4* deletion in either tissue induces spontaneous ferroptotic necrosis, which is preventable using vitamin E or liproxtatin 1 (refs. 14,189).

Systemic metabolic effects add further complexity. In models of IL-6-driven cachexia secondary to CRC and PDAC, ketogenic diets potentiate tumour ferroptosis but simultaneously induce systemic oxidative stress, deplete NADPH needed for adrenal steroidogenesis and thus accelerate cachexia onset¹⁹⁰. Such findings caution that widespread ferroptotic stress might exacerbate systemic inflammation or metabolic collapse, particularly in already catabolic patients.

Together, these findings illustrate that ferroptosis-based therapies must balance potent antitumour activity with the protection of vulnerable non-malignant cells and tissues. Future clinical translation will depend on therapeutic designs that enhance tumour specificity while minimizing collateral oxidative injury, supported by vigilant monitoring of immune, haematopoietic and organ function.

Preclinical model limitations

Many foundational ferroptosis discoveries were derived from traditional two-dimensional cancer cell line models (most notably using the ferroptosis-sensitive fibrosarcoma line HT-1080)³, which do not recapitulate key metabolic, stromal and immune features of the TME. As a result, ferroptosis sensitivities observed *in vitro* often diverge from *in vivo* responses; for example, GPX4 inhibition is uniformly lethal in two-dimensional cultures but has variable cytotoxic activity in tumour xenografts owing to pharmacokinetic constraints and microenvironmental protection²⁴.

More advanced models are required to address these gaps. Patient-derived organoids largely preserve tumour-specific heterogeneity in lipid metabolism and ferroptosis pathways, providing a more physiologically relevant platform for mechanistic and therapeutic interrogation. PDXs maintain tumour architecture and metabolic gradients but lack an intact immune system, thus limiting their utility for studying ferroptosis–immune interactions. Immunocompetent mouse models, including genetically engineered models of *Kras*-mutant lung and pancreatic cancers, enable interrogation of ferroptosis within native metabolic and immune landscapes, although species-specific differences in lipid composition, immune biology and iron handling constrain direct extrapolation to humans. Humanized mouse models are constrained by incomplete immune reconstitution and non-physiological human–mouse metabolic interactions that

might confound ferroptotic responses. Overall, these limitations highlight the need for multimodal, cross-platform evaluations to accurately assess ferroptosis-based therapies and identify the disease contexts that are most likely to be conducive to clinical benefit.

Clinical trial limitations

Despite rapid mechanistic progress, clinical testing of ferroptosis-directed therapeutic strategies remains limited. ClinicalTrials.gov lists ~20 ferroptosis-related studies, mostly focused on inflammatory or critical care indications rather than oncology. Only one active, oncology-specific trial is explicitly designed to test a therapeutic approach to modulate ferroptosis: a phase II trial evaluating temozolomide with or without the dopamine receptor D2 (DRD2) antagonist haloperidol in patients with recurrent glioblastoma (NCT06218524), based on preclinical evidence that DRD2 blockade enhances temozolomide-induced ferroptosis¹⁹¹. A completed phase I trial evaluated intratumoural delivery of carbon nanoparticles loaded with Fe²⁺ in patients with various advanced-stage solid tumours (NCT06048367), with a proposed focus on *KRAS*-mutant cancers, particularly PDAC, which is considered a ferroptosis-prone tumour type, although results have not yet been reported.

A key translational barrier is the lack of validated pharmacodynamic markers to confirm induction of ferroptosis in patients, with standard imaging, serum assays and single-time-point biopsy samples offering limited insight into lipid peroxidation or iron-dependent redox flux. Candidate plasma biomarkers such as oxidized phospholipids, labile iron measures, lipid ROS signatures and GPX4 activity remain insufficiently standardized for clinical deployment. Clinical trials are further constrained by the absence of validated predictive biomarkers that identify tumours in which ferroptosis-inducing mechanisms are likely to be effective, as well as by substantial interpatient and intratumoural heterogeneity in ferroptosis sensitivity, which complicates patient selection and might obscure signals of therapeutic efficacy.

Opportunities and emerging solutions

Despite the substantial barriers to clinical translation discussed above, several technological and conceptual advances now provide a realistic path towards harnessing ferroptosis therapeutically. These advances include new drugs and drug combinations as well as novel biomarkers and approaches for patient selection and response assessment.

New ferroptosis inducers

The pharmacological limitations of first-generation ferroptosis inducers – poor solubility, metabolic instability and dose-limiting toxicities – have driven efforts to develop new agents with improved drug-like properties and tumour specificity. Several complementary targeting strategies are now emerging.

Targeting cystine metabolism. A structure-based virtual screen for novel SLC7A11 inhibitors identified ‘compound 1’ (PubChem CID: 3492258), which has a stronger predicted binding affinity than erastin for SLC7A11 and was demonstrated to suppress cystine uptake and trigger ferroptotic death in HeLa cervical cancer cells¹⁹². Although still in preclinical development, this agent illustrates how rational small-molecule design can refine the pharmacological liabilities of first-generation system xc⁻ inhibitors.

An orthogonal approach is provided by cyst(e)inase, an engineered cystathionine γ -lyase variant optimized for degradation of extracellular cystine and cysteine to impose sustained systemic cyst(e)ine

depletion¹⁹³. Cyst(e)inase induces robust ferroptosis in vitro and in vivo, including in models of cystine-addicted PDAC²⁷. Preclinical studies in mice and non-human primates demonstrate that this agent has favourable pharmacokinetics and durable enzyme activity, mediating on-target cyst(e)ine depletion with acceptable toxicity¹⁹³. Additional studies focused on haematological malignancies, including chronic lymphocytic leukaemia, indicate that cyst(e)inase has potent antitumour activity in vitro, ex vivo and in mouse models by depleting GSH and exacerbating oxidative stress, including in settings of stromal-supported drug resistance¹⁹⁴. Although no oncology trials of cyst(e)inase have been initiated to date, early clinical development of cystine-binding thiol drugs for cyst(e)ine depletion in relevant metabolic disease indications (for example, cystinuria; NCT03663855 and NCT02125721) might provide the safety foundation for future oncology applications.

Targeting iron metabolism. Agents that interfere with iron handling can trigger ferroptosis by expanding the LIP via ferritin degradation, lysosomal destabilization, mobilization of acidic iron stores or disruption of iron–sulfur cluster biogenesis¹⁹⁵. The lysosome-selective Fe²⁺ activator fentomycin 1 exemplifies this approach. This small-molecule bifunctional compound was designed to target plasma membrane lipids, accumulate in lysosomes via endocytosis and subsequently form a redox-active iron complex that catalyses phospholipid oxidation to induce ferroptosis⁶⁴. Fentomycin 1 has been shown to selectively eliminate iron-rich, CD44-high primary sarcoma and PDAC cells and eradicate drug-tolerant persister cells (SUM159 TNBC cells resistant to doxorubicin) in vitro, and suppress intranodal tumour growth in a breast cancer metastasis model⁶⁴. However, the full in vivo pharmacology of this agent remains to be defined.

Precision modulation of GPX4 and FSP1. Novel covalent GPX4 or FSP1 inhibitors utilize electrophiles with finely tuned reactivity to achieve sustained target engagement while minimizing off-target proteome modifications^{196,197}. Rational optimization to enhance membrane penetration and pharmacokinetic properties is anticipated to improve the translational suitability of these agents compared with earlier generation lipophilic chloroacetamides⁸¹. Whereas most GPX4 inhibitors are engineered to covalently engage the crucial active-site selenocysteine residue (Sec46), a thermal-shift screen of 9,719 lead-optimized compounds identified LOC1886 as a high-affinity allosteric binder of cysteine 66 (Cys66), which induces a loop-to-helix transition that destabilizes GPX4 and triggers ferroptosis in HT-1080 cells¹⁹⁸. Although this discovery establishes the druggability of the Cys66 allosteric pocket, substantial medicinal chemistry refinement will be required to develop clinically viable GPX4 inhibitors. By contrast, the current repertoire of FSP1 inhibitors remains limited¹⁹⁷, underscoring the need for further development of selective and pharmacologically optimized agents targeting this pathway.

Targeting metabolic nodes that influence ferroptosis sensitivity. Small molecules that disrupt upstream metabolic pathways, such as glutaminolysis, the mevalonate–CoQ₁₀ axis, GSH synthesis or PUFA desaturation, can lower the ferroptotic threshold without directly inhibiting GPX4. By reshaping redox balance, phospholipid composition or NADPH availability, these agents can create a membrane environment that is more permissive to lipid peroxidation. Clinically used statins (for example, simvastatin and atorvastatin) exemplify this approach by depleting mevalonate-derived CoQ₁₀ and isopentenyl pyrophosphate, thereby weakening endogenous

lipid antioxidant defences and sensitizing tumours to ferroptosis in mouse models¹⁹⁹.

Cell type-specific ferroptosis inducers. An emerging therapeutic strategy is to trigger ferroptosis selectively in cancer cells rather than broadly inhibiting GPX4, FSP1 or SLC7A11. This strategy depends on agents that exploit tumour-specific metabolic states or receptor profiles to achieve therapeutic selectivity. For example, N6F11 binds to the RING domain of the E3 ubiquitin–ISG15 ligase TRIM25 and promotes its interaction with GPX4, thereby inducing TRIM25–E2 (UBCH5B)-dependent K48-linked ubiquitination and subsequent proteasomal degradation of GPX4, which leads to ferroptosis in tumour cells²⁰⁰. Because TRIM25 expression is low in most immune cell subsets, N6F11 elicits tumour-restricted ferroptosis without impairing antitumour immunity in mouse models of PDAC²⁰⁰.

PROTAC-based ferroptosis inducers. Proteolysis-targeting chimeras (PROTACs) provide a complementary strategy for ferroptosis activation by inducing complete degradation of GPX4 or FSP1 through the ubiquitin–proteasome system. By removing the entire protein, thereby circumventing resistance mutations and avoiding partial inhibition, which often activates compensatory antioxidant pathways, PROTACs can exert more sustained ferroptotic pressure in otherwise refractory tumours^{201,202}. The GPX4-directed PROTAC 8e triggers rapid proteasome-dependent GPX4 loss, robust lipid peroxidation and ferroptosis, with strong efficacy against *RAS*-mutant and drug-resistant cancer cells and sustained GPX4 depletion in xenografts²⁰¹. The FSP1 degrader C7 similarly sensitizes HCC cells to GPX4 inhibition, producing synergistic antitumour effects with favourable pharmacokinetic and toxicity profiles in mouse models²⁰².

Nanotechnology-enabled delivery systems. Nanomaterials offer additional control over drug potency, pharmacokinetics and tumour selectivity. Lipid nanoparticles, polymeric micelles and inorganic carriers can be engineered to co-deliver ferroptosis inducers with iron, PUFA substrates and/or immunomodulators, and to release payloads in response to tumour-specific cues such as acidity, ROS or protease activity²⁰³. Prodrug designs – activated by hypoxia, enzymes or redox stress – further confine active drug generation to the TME²⁰³. Importantly, these strategies have demonstrated antitumour activity in preclinical models; for example, iron-containing nanoparticles loaded with the ferroptosis inducer erastin suppress tumour growth in mouse models of PDAC by synergistically amplifying Fenton chemistry and erastin-induced ferroptosis, leading to enhanced lipid peroxidation and disruption of redox homeostasis²⁰⁴.

Antibody–drug conjugates. Ferroptosis-based antibody–drug conjugates (ADCs) couple tumour antigen specificity with highly potent lipid peroxidation chemistry. By directing ferroptosis-inducing payloads to defined tumour subsets, such agents enable localized cytotoxicity while limiting off-tumour injury. A cadherin 17 (CDH17)–guanylate cyclase 2C (GUCY2C) bispecific ADC exemplifies this strategy by selectively delivering the GPX4 inhibitor RSL3 to CRC cells, driving robust ferroptotic lipid peroxidation and deep tumour regression in mouse models, with improved safety over monospecific ADCs targeting the same antigens individually²⁰⁵.

Biomarker development

The clinical translation of ferroptosis-based therapies will depend on robust, multimodal biomarkers capable of predicting tumour

susceptibility and monitoring on-target activity. Genomic alterations in redox-regulatory genes (for example, *KEAPI* and *NFE2L2*), iron handling-related genes (for example, *TFRC* and *NCOA4*) and canonical tumour-suppressor genes (such as *TP53*) collectively shape the intrinsic ferroptosis vulnerability or resistance of cancer cells. Broader transcriptomic programmes reflecting system x_c^- activity, redox-buffering capacity and PUFA-PL biosynthesis have the potential to provide additional predictive granularity beyond single-gene markers²⁰⁶. Additionally, stress-response indicators such as prostaglandin G/H synthase 2 (encoded by *PTGS2*, a canonical NF- κ B target gene)²⁴ and microtubule-associated protein 1 light chain 3 (MAP1LC3; a marker of autophagic response)⁴³ are often induced during lipid peroxidation and are widely used experimentally, but their activation reflects generalized cellular stress rather than ferroptosis itself, limiting their diagnostic specificity. This complexity poses a considerable challenge for identifying clinically applicable and feasible pharmacodynamic and/or predictive biomarkers, although an improved understanding of the mechanisms and regulation of ferroptosis has presented a variety of potential candidates whose further exploration is warranted (Table 2). Nevertheless, no single marker reliably captures ferroptotic susceptibility; therefore, integrated biomarker panels that merge genomic alterations, transcriptomic programmes, metabolic and lipidomic profiles, imaging readouts and circulating indicators are likely to provide the most robust framework for patient selection and real-time monitoring.

Pharmacodynamic biomarkers. Ferroptosis is marked by characteristic metabolic shifts detectable by metabolomics and lipidomics, including expansion of the LIP, reduced GSH to oxidized GSSG ratios, accumulation of oxidized phospholipids (notably phosphatidylethanolamine hydroperoxides) and redistribution of PUFA-PLs versus MUFA-PLs^{49,207}. Because these changes arise before overt cell death, they serve as promising pharmacodynamic markers of ferroptosis induction. For example, an integrated lipidomic analysis of patient-derived glioblastoma specimens revealed that *CDKN2A* loss redirects oxidizable PUFAs from triacylglyceride stores into membrane phospholipids, thereby elevating basal levels of lipid peroxidation and creating a marked dependency on GPX4, illustrating how tumour-specific lipidomic wiring can prime cancers for ferroptosis²⁰⁸. This lipidomic state, although primarily predictive of ferroptosis susceptibility, provides a potential framework for pharmacodynamic assessment, given that treatment-induced increases in membrane lipid peroxidation products or dynamic shifts in PUFA-PL oxidation could be monitored to confirm on-target ferroptosis engagement in vivo.

Non-invasive molecular imaging offers complementary opportunities to quantify ferroptotic pharmacodynamics in vivo; PET-based tools are particularly advanced in this regard. The LIP-responsive radiotracer ¹⁸F-trioxolane (¹⁸F-TRX) enables quantitative analysis of intratumoural labile iron, as demonstrated in human glioma and renal cell carcinoma xenograft models²⁰⁹. In another preclinical study, ⁶⁸Ga-NOTA-transferrin was synthesized with high radiochemical purity and was shown to correlate with TFRC expression and sensitivity to the ferroptosis inducer erastin in renal cancer cell lines²¹⁰. Although in vitro uptake of ⁶⁸Ga-NOTA-transferrin was higher in erastin-sensitive, TFRC-high cells, preliminary xenograft experiments did not demonstrate significantly different in vivo uptake between tumours derived from these cells versus TFRC-low cells, probably owing to intratumoural heterogeneity in TFRC expression²¹⁰. (4S)-4-(3-[¹⁸F] Fluoropropyl)-L-glutamic acid (¹⁸F-FSPG), a glutamate analogue

Table 2 | Biomarkers and imaging modalities for clinical monitoring of ferroptosis

Biomarker category	Biomarker or tracer	What is measured	Specimen type	Clinical advantages and/or limitations	Refs.
Lipid peroxidation (PD)	MDA, 4-HNE adducts	End-products of PUFA-PL peroxidation	Plasma, urine, tumour biopsy samples	Widely measurable but low specificity	79
Lipid peroxidation (PD)	Oxidized PE-OOH	Direct enzymatic lipid peroxidation	Lipidomics (plasma, tumour samples)	High specificity but LC-MS-MS required	49,207
Lipid metabolism (predictive)	ACSL4 expression and/or activity	PUFA-CoA generation; ferroptosis sensitivity	Tumour biopsy samples	Tumour subtype-dependent variability in the relationship between expression or activity and ferroptosis sensitivity	47–49
Iron metabolism (predictive)	TFRC; ferritin; transferrin saturation	Tumoural iron uptake; systemic iron loading	Tumour biopsy samples; blood	Indirect measure of ferroptosis sensitivity; limited tumour specificity	39,120
Antioxidant defences (predictive)	GPX4, SLC7A11, FSP1	Core ferroptosis suppressor pathways	Tumour biopsy samples	Requires high-quality tissue	3,15, 16,24
Mitochondrial redox (PD)	Hyperoxidized PRDX3	Mitochondrial redox stress	Tumour biopsy samples	Highly specific but specialized assays needed	214
Immunomodulatory DAMPs (PD)	HMGB1, PGE ₂ , 8-OHG decorin, GPX4	Ferroptosis-associated DAMP emission	Plasma	Sensitive but non-specific	156–160, 169
Stress markers (predictive)	PTGS2, MAP1LC3	NF-κB and autophagy responses	Tumour biopsy samples	Indirect measure of ferroptosis sensitivity; context-dependent	24,43
PET imaging (PD)	¹⁸ F-TRX	Labile iron pool	NA: imaging of in situ tumours	Translational potential	209
PET imaging (PD)	⁶⁸ Ga-NOTA-Tf	TFRC expression	NA: imaging of in situ tumours	Translational potential	210
PET imaging (PD)	¹⁸ F-FSPG	System xc ⁻ activity	NA: imaging of in situ tumours	Clinically tested	211,212
MRI imaging (PD)	Art-Gd	Labile iron pool	MRI	Lower sensitivity than PET	213
Metabolic markers (PD)	Itaconate, polyamines, methylglyoxal	Metabolic rewiring	Plasma	Requires MS-based metabolomic assays	125, 130–133

4-HNE, 4-hydroxynonenal; 8-OHG, 8-hydroxyguanosine; ACSL4, long-chain fatty acid CoA ligase 4; Art-Gd, artemisinin-based gadolinium; DAMP, damage-associated molecular pattern; FSP1, ferroptosis suppressor protein 1; FSPG, florilglutamic acid; GPX4, glutathione peroxidase 4; HMGB1, high mobility group protein B1; LC-MS-MS, liquid chromatography tandem mass spectrometry; MAP1LC3, microtubule-associated protein 1 light chain 3; MDA, malondialdehyde; MS, mass spectrometry; NA, not applicable; NOTA-Tf, 2-(*p*-isothiocyanatobenzyl)-1,4,7-triazacyclononane-1,4,7-triacetic acid-conjugated human transferrin; PD, pharmacodynamic; PE-OOH, phosphatidylethanolamine hydroperoxides; PGE₂, prostaglandin E₂; PRDX3, peroxiredoxin 3; PTGS2, prostaglandin G/H synthase 2; PUFA-CoA, polyunsaturated fatty acyl coenzyme A; PUFA-PL, polyunsaturated fatty acid-containing phospholipid; SLC7A11, solute carrier family 7 member 11; TFRC, transferrin receptor protein 1; TRX, trioxolane.

transported predominantly by system xc⁻, has a favourable biodistribution and high tumour detection rates in patients with prostate cancer, with improved tumour-to-background contrast compared with ¹⁸F-fluorodeoxyglucose in several anatomical sites owing to low physiological uptake in non-malignant tissues²¹¹. ¹⁸F-FSPG has also been evaluated clinically in patients with head and neck cancer, CRC or non-Hodgkin lymphoma²¹². However, ¹⁸F-FSPG uptake reflects transporter activity rather than ferroptosis itself and might be influenced by inflammation or changes in amino acid metabolism. Molecular imaging using MRI-based probes can complement PET by offering high anatomical resolution. An artemisinin-based Fe²⁺-activated MRI contrast agent (Art-Gd) enables early detection of ferroptosis during anticancer drug-induced cardiac and renal injury in mice²¹³. Nonetheless, MRI has lower sensitivity than PET and requires adequate Fe²⁺ availability, which varies across disease states.

Circulating biomarkers provide an attractive, low-cost adjunct to imaging approaches for pharmacodynamic monitoring. Increased HMGB1, PGE₂, GPX4, decorin or DNA levels in plasma might reflect ferroptosis-associated immunosuppressive or immunostimulatory responses. However, because these mediators can also be actively secreted during inflammation or non-lethal stress, their specificity for ferroptosis is limited. In tumour biopsy samples, immunohistochemical detection of lipid peroxidation products (such as 4-HNE or

malondialdehyde) or ferroptosis regulator expression provides more direct evidence of ferroptotic stress. ACSL4 is a well-established determinant and biomarker of ferroptosis, and transgenic overexpression of this enzyme can restore ferroptotic sensitivity in otherwise resistant or metastatic cancer cells^{47,176}. TFRC was identified as a ferroptosis marker through an unbiased screen of ~4,750 antibodies as the target antigen of the ferroptosis-selective 3F3-FMA antibody, which accumulates at the plasma membrane and endosomal recycling compartment¹²⁰. Hyperoxidized peroxiredoxin 3 (PRDX3) is one of the most specific tissue biomarkers of ferroptosis: mitochondrial lipid peroxides directly trigger PRDX3 hyperoxidation, whereas apoptosis, necroptosis or generic ROS do not generate the localized lipid peroxide flux required to convert its catalytic cysteine to sulfinic/sulfonic acid²¹⁴. PRDX3 hyperoxidation was initially validated in mouse models of chronic liver diseases²¹⁴, and non-oxidized PRDX3 can act as a ferroptosis suppressor in certain tumour contexts, including ovarian cancer stem-like cells²¹⁵.

Predictive biomarkers for patient stratification and precision oncology. The substantial intertumoural heterogeneity in genetic drivers, metabolic programmes and microenvironmental states indicates that ferroptosis-directed therapies will require biomarker-guided patient selection rather than uniform application. Multiomic profiling has revealed that some cancers harbour intrinsic ferroptotic liabilities,

such as a dependence on cystine uptake, expanded PUFA-PL pools, dysregulated iron metabolism or chronic oxidative stress, whereas others acquire strong ferroptosis-suppressive circuits centred on GPX4, FSP1 or upstream metabolic pathways, establishing a foundation for tumour lineage-based and genotype-informed precision strategies^{216,217}.

A Chinese Breast Cancer Genome Atlas (CBCGA) study illustrates this principle²¹⁶. This integrative genomic, proteogenomic, metabolomic and lipidomic analysis involving a cohort of 773 patients with breast cancer identified basal-like tumours as being uniquely ferroptosis-prone, enriched for PUFA-PLs, oxidized lipids, and ACSL4 and/or TFRC expression, with matched patient-derived organoids demonstrating marked sensitivity to erastin and RSL3 (ref. 216). Beyond breast cancer, spatial multiomic analysis of matched tumour and non-malignant tissue samples from patients with ccRCC revealed conserved intratumoural gradients in cysteine–GSH flux, PUFA abundance and GPX4 activity closely linked to immune composition; these immunometabolic niches, defined by distinct metabolite signatures (including 1-methylimidazole acetate), were found to be predictive of response to anti-angiogenic agents and, therefore, could potentially be used to refine patient classification²¹⁷. Building on these frameworks, multimodal machine learning approaches that integrate lipidomic signatures, oxidized phospholipid burden, ACSL4 and/or TFRC expression, pathology and radiomics might enable the identification of patients who are most likely to benefit from ferroptosis-based interventions. Embedding such lineage-aware, multiomic biomarkers into clinical trial design will be essential to enrich for tumours with authentic ferroptosis vulnerabilities and thus maximize therapeutic efficacy.

Combination therapies

Given the complexity of tumour biology and the relatively narrow therapeutic index of ferroptosis inducers, rational combination strategies are likely to be more effective than monotherapy. Mechanistic links provide promising potential for the combination of various treatment modalities with ferroptosis inducers.

Synergy with immune checkpoint inhibitors. Ferroptosis can potentiate the activity of ICIs by enhancing tumour immunogenicity via the release of immunostimulatory DAMPs²¹⁸ (Fig. 3c). In addition, IFN γ released by ICI-activated CD8⁺ T cells suppresses system xc⁻ components via JAK1–STAT1 signalling, reducing cystine uptake, impairing GPX4 activity and thus promoting lipid peroxidation and ferroptosis in cancer cells¹⁶³ (Fig. 3d). Endogenous arachidonic acid cooperates with IFN γ to drive ACSL4-dependent cancer cell ferroptosis, as demonstrated across melanoma (Yumm5.2 and B16F10) and CRC (MC38) models, thereby amplifying CD8⁺ T cell-mediated antitumour immunity, restraining tumour progression in immunocompetent hosts and enhancing responsiveness to anti-PD-(L)1 antibodies¹⁶⁴. These immunostimulatory effects, however, must be balanced against context-specific immune cell vulnerabilities.

Excessive lipid peroxidation in DCs¹⁶² or CD8⁺ T cells^{161,179} can compromise antigen presentation and effector function, and certain ferroptotic settings (such as exosomal release of KRAS-G12D as a result of autophagy-dependent ferroptosis) can promote M2-like, pro-tumour macrophage polarization²¹⁹. Moreover, ferroptosis in cancer cells can indirectly impair DC maturation and activation, in part via the release of immunosuppressive DAMPs, including GPX4 (ref. 160) (Fig. 3c). Consistent with a combinatorial strategy, antibody-mediated targeting of extracellular GPX4, which blocks GPX4 binding to ZP3 on DCs, enhances the antitumour activity of ICIs in models of PDAC¹⁶⁰.

Tumour–immune metabolic checkpoints can further constrain the therapeutic activity of ICIs and might also influence responses to ferroptosis-based interventions. In TNBC, a tumour–macrophage metabolic checkpoint has been described whereby cancer cells upregulate the expression of haem-binding protein 2 (HEBP2) to activate a forkhead box A1 (FOXA1)–GST- π 1 (GSTP1) axis and out-compete C–C motif chemokine ligand 3 (CCL3)-positive macrophages for glutamine, thus inducing macrophage ferroptosis and thereby suppressing antitumour immunity and limiting responsiveness to PD-1 blockade²²⁰. Importantly, this study also revealed that genetic or pharmacological inhibition of GSTP1 restores macrophage fitness and enhances the antitumour activity of ICIs, although whether ferroptosis inducers enhance antitumour immunity was not evaluated²²⁰. Rather, the findings imply that non-selective ferroptosis induction might exacerbate immunosuppression by promoting ferroptotic loss of antitumour immune cells²²⁰. Finally, acyl-CoA-binding protein (ACBP; also known as diazepam-binding inhibitor) has been identified as a pro-carcinogenic factor in HCC: genetic, receptor-based or immunological inhibition of ACBP suppresses oncogenic and ferroptosis-regulatory transcriptional programmes, increases tumour sensitivity to ferroptosis induction and improves responses to anti-PD-1 antibodies in mouse models²²¹.

Together, these findings underscore a therapeutic duality in ferroptosis–ICI combinations. The timing and dosing of ferroptosis inducers relative to ICIs are likely to be crucial factors, given that excessive or mistimed ferroptotic stress can impair DC and CD8⁺ T cell function, and might also compromise tumour-suppressive CCL3⁺ macrophage populations, whereas appropriately calibrated ferroptosis induction enhances tumour immunogenicity and antitumour immunity. Optimizing treatment sequence, intensity and tumour context will therefore be essential to maximizing benefit while minimizing immune suppression.

Synergy with radiotherapy. Apoptosis has long been considered the predominant mode of radiation-induced cancer cell death, and defects in apoptotic signalling are a well-recognized mechanism of radioresistance. However, ionizing radiation can also trigger ferroptosis in cancer cells²²². In preclinical models, radiation promotes lipid peroxidation and perturbs antioxidant defences, thereby lowering the threshold for ferroptotic death²²³. By engaging this parallel vulnerability, ferroptosis enhances radiosensitivity, and combining radiotherapy with ferroptosis inducers has shown synergistic antitumour effects in radioresistant models^{223,224}. Data from another study demonstrate that inhibition of ETC complex I via genetic deletion of NADH–ubiquinone oxidoreductase core subunit S2 (*NDUFS2*) sensitizes cancer cells to GPX4 inhibitor-induced ferroptosis by depleting ubiquinol (CoQH₂) without triggering compensatory AMPK activation²²⁵. By contrast, acute pharmacological inhibition of ETC complex I reduces CoQH₂ levels but concomitantly activates AMPK owing to energy stress, which imposes a ferroptosis-suppressive brake and limits overall sensitivity²²⁵. Importantly, in AMPK-inactive or *STK11*-deficient tumour models – including HT-1080 fibrosarcoma cells, *STK11*-mutant lung cancer PDXs and syngeneic LKR-13 tumours – pharmacological inhibition of ETC complex I overcomes this constraint, synergizes with radiotherapy and suppresses tumour growth via enhanced lipid peroxidation and ferroptosis²²⁵. A drawback with these combination strategies is that ferroptosis might also be induced in non-malignant cells, which could lead to additional toxicities.

Synergy with targeted therapies. Oncoprotein-targeted agents, including inhibitors of KRAS, EGFR and BRAF, as well as multitarget anti-angiogenic tyrosine kinase inhibitors (TKIs), can remodel tumour metabolism, elevate oxidative stress or activate compensatory antioxidant circuits, thereby creating context-dependent ferroptosis vulnerabilities¹². In *EGFR*-mutant NSCLC, intrinsic and acquired resistance to EGFR TKIs is associated with heightened sensitivity to ferroptosis induction; co-targeting SLC7A11 using erastin, particularly in combination with epigenetic agents such as the histone deacetylase inhibitor vorinostat (which downregulates system xc⁻ expression), further enhances ferroptotic death in vitro and in xenograft models²²⁶. A similar dependency emerges in glioblastoma, whereby EGFR signalling suppresses ferroptosis by enhancing nuclear retention of the RNA N⁶-methyladenosine demethylase ALKBH5 and thereby post-transcriptionally upregulating expression of the GSH biosynthetic enzyme GCLM²²⁷. Accordingly, dual inhibition of EGFR and ALKBH5 (or GCLM) produces synergistic antitumour effects in preclinical models²²⁷, illustrating how receptor tyrosine kinase blockade can unmask ferroptosis liabilities.

In *BRAF*^{V600E}-mutant melanoma, vemurafenib-treated persister cells undergo metabolic and transcriptional reprogramming that increases dependence on GPX4, rendering them exquisitely susceptible to ferroptosis; combining BRAF inhibition with ferroptosis inducers reduces persister cell pools and delays disease relapse in preclinical models¹⁰. *KRAS*-mutant tumours similarly rewire cystine–GSH metabolism and antioxidant defences, and inducing ferroptosis via ALDH1A1 inhibition or augmentation of spermidine–spermine N1-acetyltransferase 1 (SAT1; also known as diamine acetyltransferase 1)-driven polyamine catabolism enhances the activity of KRAS-G12C inhibitors across cell lines, patient-derived organoids and mouse models^{228,229}.

Therapy resistance in CRC can occur via a distinct lineage-specific mechanism, with prolonged 5-fluorouracil, cisplatin or SN-38 exposure yielding drug-persistent clones that express high levels of leucine-rich repeat containing G-protein-coupled receptor 4 (LGR4), which activates WNT– β -catenin signalling that transcriptionally upregulates SLC7A11 and thus maintains GSH biosynthesis²³⁰. Antibody-mediated LGR4 blockade disrupts this signalling axis, lowers GSH levels and restores ferroptotic sensitivity in organoid and mouse xenograft models²³⁰. Although demonstrated in the context of chemotherapy resistance, further investigation of the possible contribution of this LGR4–WNT–SLC7A11 axis to resistance to targeted therapies that impose sustained metabolic or oxidative stress is warranted.

Anti-angiogenic TKIs such as sorafenib provide another means of synergy. Although sorafenib can impair GPX4 expression and deplete GSH, resistance to this agent commonly arises through NRF2 activation and macropinocytosis-dependent cysteine acquisition; therefore, the combination of sorafenib with ferroptosis inducers or macropinocytosis inhibitors is a promising strategy to overcome this redox adaptation²³¹. In PDX models of acute myeloid leukaemia (AML), the telomerase inhibitor imetelstat acts as a lipophagy-driven ferroptosis inducer via upregulation of ACSL4 and fatty acid desaturase 2 (FADS2) activity, with *NRAS*-mutant and oxidative-stress-high AML showing the most durable responses²³². Sequential chemotherapy further primes AML cells for imetelstat-induced ferroptosis and improves disease control²³².

Collectively, these studies show that oncogenic signalling, metabolic rewiring and therapy-induced stress create actionable ferroptosis dependencies, and that rational co-targeting has the potential to deepen and prolong responses to targeted therapies, particularly by eliminating drug-tolerant persister cells^{10,11}.

Modulating lipid metabolism. Pharmacological targeting of lipid metabolism can markedly increase the sensitivity of cancer cells to ferroptosis. Inhibition of SCD1 depletes MUFAs that protect cell membranes from peroxidation, shifts phospholipid composition towards PUFA-rich species²³³ and suppresses the AKT–glycogen synthase kinase 3 β (GSK3 β)–NRF2–SLC7A11 antioxidant axis, collectively lowering the ferroptotic threshold across diverse cancer models²³⁴. Similarly, inhibition of fatty acid synthase (FASN) restricts de novo lipogenesis, thus limiting membrane remodelling and redox buffering capacity, thereby potentiating ferroptosis²³⁵. Targeting the mevalonate pathway sensitizes tumours to ferroptosis by reducing isoprenoid, squalene and CoQ₁₀ biosynthesis and impairing selenocysteine tRNA maturation required for GPX4 production (Fig. 2), collectively disabling key ferroptosis resistance mechanisms²³⁶.

Additional vulnerabilities arise from blocking pathways that regulate ether lipid synthesis, lipid droplet biogenesis or PUFA sequestration, which cancer cells use to shield PUFA-PLs from peroxidation. Inhibiting these processes expands the pool of oxidizable PUFA-PLs and intensifies ferroptotic cell death⁷¹. Such metabolic interventions might be particularly effective in malignancies with pronounced lipogenic programmes (for example, SREBP1/2-driven cancers)²³⁷ or those that rely heavily on exogenous lipid uptake (such as HCC)²³⁸, indicating clinical settings in which metabolic rewiring can potentially be exploited to strengthen ferroptosis-based therapeutic strategies.

Roadmap for clinical translation

Similar to other regulated cell death modalities, ferroptosis functions as a context-dependent determinant of tumour evolution, exerting tumour-promoting or tumour-suppressive effects depending on timing, intensity and tissue (micro)environment. Accordingly, ferroptosis regulation is highly heterogeneous, with most pathways shaped by cellular lineage, metabolic wiring and microenvironmental cues. This heterogeneity suggests that uniform approaches to ferroptosis induction, applied without biomarker-based patient selection, are likely to have limited clinical potential across diverse patient populations, rather than reflecting a lack of intrinsic therapeutic promise⁴. Emerging evidence supports the concept of ferroptotic signalling, whereby sublethal lipid peroxidation can reprogramme iron-mediated and lipid-dependent transcriptional networks – illustrated, for example, in adipose tissue²³⁹ – and alter tissue or microenvironmental states independently of overt cell death, thereby expanding the functional scope of ferroptosis beyond direct cancer cell killing.

Despite the rapid expansion of preclinical studies of ferroptosis, translation into oncology applications remains constrained by several key bottlenecks, including the lack of tumour-selective or tissue-targeted ferroptosis modulators with favourable pharmacokinetics, the absence of clinically validated biomarkers for patient stratification and pharmacodynamic monitoring, an incomplete understanding of the mechanisms of ferroptosis resistance in relapsed and/or refractory tumours, and limitations of existing preclinical models in capturing human tumour–immune–metabolic interactions. Overcoming these barriers will be essential for realizing the therapeutic potential of ferroptosis.

A focused translational framework is therefore required. Evaluations in physiologically informed models that integrate lipid metabolism, iron biology and immune context will be crucial to define tumour settings in which ferroptosis can be safely and selectively engaged. In parallel, development and clinical validation of multimodal biomarkers will be necessary to identify ferroptosis dependency and guide patient selection.

Early-phase trials testing ferroptosis-based therapies should prioritize mechanism-based end points and rational combination designs rather than ferroptosis induction as a stand-alone cytotoxic strategy.

Clinically, ferroptosis-based interventions are most plausibly deployed as context-dependent combinatorial or priming approaches, to overcome apoptosis resistance, sensitize tumours to immunotherapy or chemotherapy, constrain metastatic outgrowth, or lower therapeutic thresholds in refractory disease. Careful optimization of treatment sequencing, dosing and tumour context will be essential, given that excessive or mistimed ferroptotic stress might compromise immune function or non-malignant tissue physiology, thereby increasing toxicity risks and potentially restricting antitumour activity.

Conclusions

Overall, ferroptosis holds promise as a therapeutic axis for addressing drug resistance, metabolic plasticity and immune evasion. Aligning mechanistic insights with precision delivery, biomarker-guided patient stratification and rational combination strategies are key to advancing ferroptosis from an experimental concept to clinically actionable cancer therapy.

Published online: 24 February 2026

References

- Galluzzi, L., Kepp, O., Zitvogel, L., Tang, D. & Kroemer, G. Cancer cell death: cell-autonomous and immunogenic dimensions. *Cancer Cell* **44**, 281–305 (2026).
- Dolma, S., Lessnick, S. L., Hahn, W. C. & Stockwell, B. R. Identification of genotype-selective antitumor agents using synthetic lethal chemical screening in engineered human tumor cells. *Cancer Cell* **3**, 285–296 (2003).
- Dixon, S. J. et al. Ferroptosis: an iron-dependent form of nonapoptotic cell death. *Cell* **149**, 1060–1072 (2012).
- Dai, E. et al. A guideline on the molecular ecosystem regulating ferroptosis. *Nat. Cell Biol.* **26**, 1447–1457 (2024).
- Xue, Q. et al. Copper-dependent autophagic degradation of GPX4 drives ferroptosis. *Autophagy* **19**, 1982–1996 (2023).
- Chen, J. et al. Unusual iron-independent ferroptosis-like cell death induced by photoactivation of a typical iridium complex for hypoxia photodynamic therapy. *ACS Appl. Mater. Interfaces* **17**, 5684–5694 (2025).
- Stockwell, B. R. Ferroptosis turns 10: emerging mechanisms, physiological functions, and therapeutic applications. *Cell* **185**, 2401–2421 (2022).
- Song, X. et al. Cytosolic cytochrome c represses ferroptosis. *Cell Metab.* **37**, 1326–1343.e10 (2025).
- Tang, Q. et al. Bim- and Bax-mediated mitochondrial pathway dominates abiraterone-induced apoptosis and ferroptosis. *Free. Radic. Biol. Med.* **180**, 198–209 (2022).
- Hangauer, M. J. et al. Drug-tolerant persister cancer cells are vulnerable to GPX4 inhibition. *Nature* **551**, 247–250 (2017).
- Viswanathan, V. S. et al. Dependency of a therapy-resistant state of cancer cells on a lipid peroxidase pathway. *Nature* **547**, 453–457 (2017).
- Chen, X., Kang, R., Kroemer, G. & Tang, D. Broadening horizons: the role of ferroptosis in cancer. *Nat. Rev. Clin. Oncol.* **18**, 280–296 (2021).
- Wahida, A. & Conrad, M. Decoding ferroptosis for cancer therapy. *Nat. Rev. Cancer* **25**, 910–924 (2025).
- Friedmann Angeli, J. P. et al. Inactivation of the ferroptosis regulator Gpx4 triggers acute renal failure in mice. *Nat. Cell Biol.* **16**, 1180–1191 (2014).
- Doll, S. et al. FSP1 is a glutathione-independent ferroptosis suppressor. *Nature* **575**, 693–698 (2019).
- Bersuker, K. et al. The CoQ oxidoreductase FSP1 acts parallel to GPX4 to inhibit ferroptosis. *Nature* **575**, 688–692 (2019).
- Mao, C. et al. DHODH-mediated ferroptosis defence is a targetable vulnerability in cancer. *Nature* **593**, 586–590 (2021).
- Soula, M. et al. Metabolic determinants of cancer cell sensitivity to canonical ferroptosis inducers. *Nat. Chem. Biol.* **16**, 1351–1360 (2020).
- Kraft, V. A. N. et al. GTP cyclohydrolase 1/tetrahydrobiopterin counteract ferroptosis through lipid remodeling. *ACS Cent. Sci.* **6**, 41–53 (2020).
- Mishima, E. et al. A non-canonical vitamin K cycle is a potent ferroptosis suppressor. *Nature* **608**, 778–783 (2022).
- Kolbrink, B. et al. Vitamin K1 inhibits ferroptosis and counteracts a detrimental effect of phenprocoumon in experimental acute kidney injury. *Cell Mol. Life Sci.* **79**, 387 (2022).
- Wu, Z. et al. Hydropersulfides inhibit lipid peroxidation and protect cells from ferroptosis. *J. Am. Chem. Soc.* **144**, 15825–15837 (2022).
- Chidley, C. et al. A CRISPRi/a screening platform to study cellular nutrient transport in diverse microenvironments. *Nat. Cell Biol.* **26**, 825–838 (2024).
- Yang, W. S. et al. Regulation of ferroptotic cancer cell death by GPX4. *Cell* **156**, 317–331 (2014).
- Zou, Y. et al. A GPX4-dependent cancer cell state underlies the clear-cell morphology and confers sensitivity to ferroptosis. *Nat. Commun.* **10**, 1617 (2019).
- Xie, Y., Kang, R., Klionsky, D. J. & Tang, D. GPX4 in cell death, autophagy, and disease. *Autophagy* **19**, 2621–2638 (2023).
- Badgley, M. A. et al. Cysteine depletion induces pancreatic tumor ferroptosis in mice. *Science* **368**, 85–89 (2020).
- Zhou, N. et al. SLC7A11 is an unconventional H⁺ transporter in lysosomes. *Cell* **188**, 3441–3458.e25 (2025).
- Yang, J. S. et al. ALDH7A1 protects against ferroptosis by generating membrane NADH and regulating FSP1. *Cell* **188**, 2569–2585.e20 (2025).
- Dai, E. et al. ALFM2 blocks ferroptosis independent of ubiquinol metabolism. *Biochem. Biophys. Res. Commun.* **523**, 966–971 (2020).
- Lange, M. et al. FSP1-mediated lipid droplet quality control prevents neutral lipid peroxidation and ferroptosis. *Nat. Cell Biol.* **27**, 1902–1913 (2025).
- Palma, M. et al. Lymph node environment drives FSP1 targetability in metastasizing melanoma. *Nature* **649**, 477–486 (2026).
- Emmanuel, N., Li, H., Chen, J. & Zhang, Y. FSP1, a novel KEAP1/NRF2 target gene regulating ferroptosis and radioresistance in lung cancers. *Oncotarget* **13**, 1136–1139 (2022).
- Takahashi, N. et al. 3D culture models with CRISPR screens reveal hyperactive NRF2 as a prerequisite for spheroid formation via regulation of proliferation and ferroptosis. *Mol. Cell* **80**, 828–844.e6 (2020).
- Sun, X. et al. Activation of the p62-Keap1-NRF2 pathway protects against ferroptosis in hepatocellular carcinoma cells. *Hepatology* **63**, 173–184 (2016).
- Sun, X. et al. Metallothionein-1G facilitates sorafenib resistance through inhibition of ferroptosis. *Hepatology* **64**, 488–500 (2016).
- Yan, B. et al. Membrane damage during ferroptosis is caused by oxidation of phospholipids catalyzed by the oxidoreductases POR and CYB5R1. *Mol. Cell* **81**, 355–369 (2021).
- Zou, Y. et al. Cytochrome P450 oxidoreductase contributes to phospholipid peroxidation in ferroptosis. *Nat. Chem. Biol.* **16**, 302–309 (2020).
- Hou, W. et al. Autophagy promotes ferroptosis by degradation of ferritin. *Autophagy* **12**, 1425–1428 (2016).
- Gao, M. et al. Ferroptosis is an autophagic cell death process. *Cell Res.* **26**, 1021–1032 (2016).
- Muller, S. et al. CD44 regulates epigenetic plasticity by mediating iron endocytosis. *Nat. Chem. Biol.* **12**, 929–938 (2020).
- Wang, Y., Liu, Y., Liu, J., Kang, R. & Tang, D. NEDD4L-mediated LTF protein degradation limits ferroptosis. *Biochem. Biophys. Res. Commun.* **531**, 581–587 (2020).
- Li, J. et al. Tumor heterogeneity in autophagy-dependent ferroptosis. *Autophagy* **17**, 3361–3374 (2021).
- Liu, J. et al. NUPR1 is a critical repressor of ferroptosis. *Nat. Commun.* **12**, 647 (2021).
- Zhuang, X. et al. Ageing limits stemness and tumorigenesis by reprogramming iron homeostasis. *Nature* **637**, 184–194 (2025).
- Yu, Y. et al. Hepatic transferrin plays a role in systemic iron homeostasis and liver ferroptosis. *Blood* **136**, 726–739 (2020).
- Yuan, H., Li, X., Zhang, X., Kang, R. & Tang, D. Identification of ACSL4 as a biomarker and contributor of ferroptosis. *Biochem. Biophys. Res. Commun.* **478**, 1338–1343 (2016).
- Doll, S. et al. ACSL4 dictates ferroptosis sensitivity by shaping cellular lipid composition. *Nat. Chem. Biol.* **13**, 91–98 (2017).
- Kagan, V. E. et al. Oxidized arachidonic and adrenic PEs navigate cells to ferroptosis. *Nat. Chem. Biol.* **13**, 81–90 (2017).
- Zhang, H. L. et al. PKC β phosphorylates ACSL4 to amplify lipid peroxidation to induce ferroptosis. *Nat. Cell Biol.* **24**, 88–98 (2022).
- Magtanong, L. et al. Exogenous monounsaturated fatty acids promote a ferroptosis-resistant cell state. *Cell Chem. Biol.* **26**, 420–432.e29 (2019).
- Luis, G. et al. Tumor resistance to ferroptosis driven by stearoyl-CoA desaturase-1 (SCD1) in cancer cells and fatty acid binding protein-4 (FABP4) in tumor microenvironment promote tumor recurrence. *Redox Biol.* **43**, 102006 (2021).
- Li, Z. et al. LPCAT1-mediated membrane phospholipid remodelling promotes ferroptosis evasion and tumour growth. *Nat. Cell Biol.* **26**, 811–824 (2024).
- Lin, Z. et al. The lipid flippase SLC47A1 blocks metabolic vulnerability to ferroptosis. *Nat. Commun.* **13**, 7965 (2022).
- Gao, M. et al. Role of mitochondria in ferroptosis. *Mol. Cell* **73**, 354–363.e3 (2019).
- Gao, M., Monian, P., Quadri, N., Ramasamy, R. & Jiang, X. Glutaminolysis and transferrin regulate ferroptosis. *Mol. Cell* **59**, 298–308 (2015).
- Qiu, B. et al. Phospholipids with two polyunsaturated fatty acyl tails promote ferroptosis. *Cell* **187**, 1177–1190.e18 (2024).
- Deshwal, S. et al. Mitochondria regulate intracellular coenzyme Q transport and ferroptotic resistance via STAR7D. *Nat. Cell Biol.* **25**, 246–257 (2023).
- Mishima, E. et al. DHODH inhibitors sensitize to ferroptosis by FSP1 inhibition. *Nature* **619**, E9–E18 (2023).
- Guo, W. et al. Mitochondrial CCN1 drives ferroptosis via fatty acid β -oxidation. *Dev. Cell* **60**, 2294–2312 (2025).
- Liang, F. G. et al. OPA1 promotes ferroptosis by augmenting mitochondrial ROS and suppressing an integrated stress response. *Mol. Cell* **84**, 3098–3114.e6 (2024).

62. Li, C., Liu, J., Hou, W., Kang, R. & Tang, D. STING1 promotes ferroptosis through MFN1/2-dependent mitochondrial fusion. *Front. Cell Dev. Biol.* **9**, 698679 (2021).
63. Liu, X. et al. Endocytosis is essential for cysteine-deprivation-induced ferroptosis. *Mol. Cell* **85**, 3333–3342.e4 (2025).
64. Canequé, T. et al. Activation of lysosomal iron triggers ferroptosis in cancer. *Nature* **642**, 492–500 (2025).
65. Gao, H. et al. Ferroptosis is a lysosomal cell death process. *Biochem. Biophys. Res. Commun.* **503**, 1550–1556 (2018).
66. Swanda, R. V. et al. Lysosomal cystine governs ferroptosis sensitivity in cancer via cysteine stress response. *Mol. Cell* **83**, 3347–3359.e9 (2023).
67. Armenta, D. A. et al. Ferroptosis inhibition by lysosome-dependent catabolism of extracellular protein. *Cell Chem. Biol.* **29**, 1588–1600.e7 (2022).
68. von Krusenstiern, A. N. et al. Identification of essential sites of lipid peroxidation in ferroptosis. *Nat. Chem. Biol.* **19**, 719–730 (2023).
69. Sassano, M. L. et al. Endoplasmic reticulum-mitochondria contacts are prime hotspots of phospholipid peroxidation driving ferroptosis. *Nat. Cell Biol.* **27**, 902–917 (2025).
70. Zou, Y. et al. Plasticity of ether lipids promotes ferroptosis susceptibility and evasion. *Nature* **585**, 603–608 (2020).
71. Bai, Y. et al. Lipid storage and lipophagy regulates ferroptosis. *Biochem. Biophys. Res. Commun.* **508**, 997–1003 (2019).
72. Riegman, M. et al. Ferroptosis occurs through an osmotic mechanism and propagates independently of cell rupture. *Nat. Cell Biol.* **22**, 1042–1048 (2020).
73. Co, H. K. C., Wu, C. C., Lee, Y. C. & Chen, S. H. Emergence of large-scale cell death through ferroptotic trigger waves. *Nature* **631**, 654–662 (2024).
74. Ramos, S., Hartenian, E., Santos, J. C., Walch, P. & Broz, P. NIN1 induces plasma membrane rupture and release of damage-associated molecular pattern molecules during ferroptosis. *EMBO J.* **43**, 1164–1186 (2024).
75. Kayagaki, N. et al. NIN1 mediates plasma membrane rupture during lytic cell death. *Nature* **591**, 131–136 (2021).
76. Hirata, Y. et al. Lipid peroxidation increases membrane tension, Piezo1 gating, and cation permeability to execute ferroptosis. *Curr. Biol.* **33**, 1282–1294.e5 (2023).
77. Dai, E., Meng, L., Kang, R., Wang, X. & Tang, D. ESCRT-III-dependent membrane repair blocks ferroptosis. *Biochem. Biophys. Res. Commun.* **522**, 415–421 (2020).
78. Wu, J. et al. Intercellular interaction dictates cancer cell ferroptosis via NF2-YAP signalling. *Nature* **572**, 402–406 (2019).
79. Chen, X. et al. A noncanonical function of EIF4E limits ALDH1B1 activity and increases susceptibility to ferroptosis. *Nat. Commun.* **13**, 6318 (2022).
80. Yang, W. S. & Stockwell, B. R. Synthetic lethal screening identifies compounds activating iron-dependent, nonapoptotic cell death in oncogenic-RAS-harboring cancer cells. *Chem. Biol.* **15**, 234–245 (2008).
81. Eaton, J. K. et al. Selective covalent targeting of GPX4 using masked nitrile-oxide electrophiles. *Nat. Chem. Biol.* **16**, 497–506 (2020).
82. Cheff, D. M. et al. The ferroptosis inducing compounds RSL3 and ML162 are not direct inhibitors of GPX4 but of TXNRD1. *Redox Biol.* **62**, 102703 (2023).
83. Ren, X. et al. Programmable melanoma-targeted radio-immunotherapy via fusogenic liposomes functionalized with multivariate-gated aptamer assemblies. *Nat. Commun.* **15**, 5035 (2024).
84. Herrick, W. G. et al. Potent ferroptosis agent RSL3 induces cleavage of pyroptosis-specific gasdermins in cancer cells. *Sci. Rep.* **15**, 25249 (2025).
85. DeAngelo, S. L. et al. Recharacterization of the tumor suppressive mechanism of RSL3 identifies the selenoproteome as a druggable pathway in colorectal cancer. *Cancer Res.* **85**, 2788–2804 (2025).
86. Zhang, Y. et al. Imidazole ketone erastin induces ferroptosis and slows tumor growth in a mouse lymphoma model. *Cell Chem. Biol.* **26**, 623–633.e9 (2019).
87. Nakamura, T. et al. Phase separation of FSP1 promotes ferroptosis. *Nature* **619**, 371–377 (2023).
88. Nakamura, T. et al. Integrated chemical and genetic screens unveil FSP1 mechanisms of ferroptosis regulation. *Nat. Struct. Mol. Biol.* **30**, 1806–1815 (2023).
89. Hendricks, J. M. et al. Identification of structurally diverse FSP1 inhibitors that sensitize cancer cells to ferroptosis. *Cell Chem. Biol.* **30**, 1090–1103.e7 (2023).
90. Salem, S. et al. Targeting FSP1 to induce ferroptosis in chromophobe renal cell carcinoma. *Oncogene* **44**, 4075–4086 (2025).
91. Wu, K. et al. Targeting FSP1 triggers ferroptosis in lung cancer. *Nature* **649**, 487–495 (2026).
92. Liu, J., Kang, R. & Tang, D. Adverse effects of ferroptotic therapy: mechanisms and management. *Trends Cancer* **10**, 417–429 (2024).
93. Ge, C. et al. Emerging mechanisms and disease implications of ferroptosis: potential applications of natural products. *Front. Cell Dev. Biol.* **9**, 774957 (2021).
94. Crippa, V. et al. Integrative analysis of KEAP1/NFE2L2 alterations across 3600+ tumors reveals an NRF2 expression signature as a prognostic biomarker in cancer. *NPJ Precis. Oncol.* **9**, 291 (2025).
95. Wohlhieter, C. A. et al. Concurrent mutations in STK11 and KEAP1 promote ferroptosis protection and SCD1 Dependence in lung cancer. *Cell Rep.* **33**, 108444 (2020).
96. Shimura, T. et al. The prognostic importance of the negative regulators of ferroptosis, GPX4 and HSPB1, in patients with colorectal cancer. *Oncol. Lett.* **29**, 144 (2025).
97. Li, X., Zhu, M. & Dong, R. Ferroptosis's master switch GPX4 emerges as universal biomarker for precision immunotherapy: a pan-cancer study with in vitro experiments validation. *Front. Oncol.* **15**, 1643235 (2025).
98. Koppula, P. et al. A targetable CoQ-FSP1 axis drives ferroptosis- and radiation-resistance in KEAP1 inactive lung cancers. *Nat. Commun.* **13**, 2206 (2022).
99. Jiang, L. et al. Ferroptosis as a p53-mediated activity during tumour suppression. *Nature* **520**, 57–62 (2015).
100. Yang, X. et al. Regulation of VKORC1L1 is critical for p53-mediated tumor suppression through vitamin K metabolism. *Cell Metab.* **35**, 1474–1490.e8 (2023).
101. Xie, Y. et al. The tumor suppressor p53 limits ferroptosis by blocking DPP4 activity. *Cell Rep.* **20**, 1692–1704 (2017).
102. Su, Z. et al. Specific regulation of BACH1 by the hotspot mutant p53(R175H) reveals a distinct gain-of-function mechanism. *Nat. Cancer* **4**, 564–581 (2023).
103. Yagoda, N. et al. RAS-RAF-MEK-dependent oxidative cell death involving voltage-dependent anion channels. *Nature* **447**, 864–868 (2007).
104. Andreani, C., Bartolacci, C. & Scaglioni, P. P. Ferroptosis: a specific vulnerability of RAS-driven cancers? *Front. Oncol.* **12**, 923915 (2022).
105. Lei, G. et al. BRCA1 mediated dual regulation of ferroptosis exposes a vulnerability to GPX4 and PARP co-inhibition in BRCA1-deficient cancers. *Cancer Discov.* **14**, 1476–1495 (2024).
106. Alborzinia, H. et al. MYCN mediates cysteine addiction and sensitizes neuroblastoma to ferroptosis. *Nat. Cancer* **3**, 471–485 (2022).
107. Zhang, Y. et al. BAP1 links metabolic regulation of ferroptosis to tumour suppression. *Nat. Cell Biol.* **20**, 1181–1192 (2018).
108. Liu, Y., Wang, Y., Liu, J., Kang, R. & Tang, D. Interplay between MTOR and GPX4 signaling modulates autophagy-dependent ferroptotic cancer cell death. *Cancer Gene Ther.* **28**, 55–63 (2021).
109. Yi, J., Zhu, J., Wu, J., Thompson, C. B. & Jiang, X. Oncogenic activation of PI3K-AKT-mTOR signaling suppresses ferroptosis via SREBP-mediated lipogenesis. *Proc. Natl Acad. Sci. USA* **117**, 31189–31197 (2020).
110. Zhang, Y. et al. mTORC1 couples cyst(e)ine availability with GPX4 protein synthesis and ferroptosis regulation. *Nat. Commun.* **12**, 1589 (2021).
111. Conlon, M. et al. A compendium of kinetic modulatory profiles identifies ferroptosis regulators. *Nat. Chem. Biol.* **17**, 665–674 (2021).
112. Hua, Y. et al. Targeting SLC7A11-mediated cysteine metabolism for the treatment of trastuzumab-resistant HER2-positive breast cancer. *eLife* **14**, RP103953 (2025).
113. Zhang, M. et al. PRMT5-mediated arginine methylation of ACSL4 attenuates its stability and suppresses ferroptosis in renal cancer. *Research* **8**, 0789 (2025).
114. Schmitt, A. et al. BRD4 inhibition sensitizes diffuse large B-cell lymphoma cells to ferroptosis. *Blood* **142**, 1143–1155 (2023).
115. Wang, Y. et al. Histone demethylase KDM3B protects against ferroptosis by upregulating SLC7A11. *FEBS Open Bio* **10**, 637–643 (2020).
116. Luo, M. et al. miR-137 regulates ferroptosis by targeting glutamine transporter SLC1A5 in melanoma. *Cell Death Differ.* **25**, 1457–1472 (2018).
117. Song, K. et al. Plasticity of extrachromosomal and intrachromosomal BRAF amplifications in overcoming targeted therapy dosage challenges. *Cancer Discov.* **12**, 1046–1069 (2022).
118. He, Y. et al. Multi-omics characterization and therapeutic liability of ferroptosis in melanoma. *Signal. Transduct. Target. Ther.* **7**, 268 (2022).
119. Klasson, T. D. et al. ACSL3 regulates lipid droplet biogenesis and ferroptosis sensitivity in clear cell renal cell carcinoma. *Cancer Metab.* **10**, 14 (2022).
120. Feng, H. et al. Transferrin receptor is a specific ferroptosis marker. *Cell Rep.* **30**, 3411–3423.e7 (2020).
121. Singhal, R. et al. HIF-2α activation potentiates oxidative cell death in colorectal cancers by increasing cellular iron. *J. Clin. Invest.* **131**, e143691 (2021).
122. Calhoun, D. et al. Glycosaminoglycan-driven lipoprotein uptake protects tumours from ferroptosis. *Nature* **644**, 799–808 (2025).
123. Yang, C. et al. De novo pyrimidine biosynthetic complexes support cancer cell proliferation and ferroptosis defence. *Nat. Cell Biol.* **25**, 836–847 (2023).
124. Gentric, G. et al. PML-regulated mitochondrial metabolism enhances chemosensitivity in human ovarian cancers. *Cell Metab.* **29**, 156–173.e10 (2019).
125. Zhang, X. et al. Targeting ethylglyoxal metabolism to enhance ferroptosis sensitivity in tumor therapy. *Adv. Sci.* **12**, e05356 (2025).
126. Li, Y. et al. 7-Dehydrocholesterol dictates ferroptosis sensitivity. *Nature* **626**, 411–418 (2024).
127. Freitas, F. P. et al. 7-Dehydrocholesterol is an endogenous suppressor of ferroptosis. *Nature* **626**, 401–410 (2024).
128. Urano, Y., Iwagaki, A., Takeishi, A., Uchiyama, N. & Noguchi, N. Downregulation of the SREBP pathways and disruption of redox status by 25-hydroxycholesterol predispose cells to ferroptosis. *Free. Radic. Biol. Med.* **228**, 319–328 (2025).
129. Wu, R., Liu, J., Tang, D. & Kang, R. The dual role of ACO1 in inflammation. *J. Immunol.* **211**, 518–526 (2023).
130. Lin, H. et al. Itaconate transporter SLC13A3 impairs tumor immunity via endowing ferroptosis resistance. *Cancer Cell* **42**, 2032–2044.e6 (2024).
131. Zhao, Y. et al. Neutrophils resist ferroptosis and promote breast cancer metastasis through aconitate decarboxylase 1. *Cell Metab.* **35**, 1688–1703.e10 (2023).
132. Liu, K. et al. Induction of autophagy-dependent ferroptosis to eliminate drug-tolerant human retinoblastoma cells. *Cell Death Dis.* **13**, 521 (2022).
133. Sharma, P. et al. Polyamines buffer labile iron to suppress ferroptosis. Preprint at <https://www.biorxiv.org/content/10.1101/2025.06.30.662349v1> (2025).
134. Tsoi, J. et al. Multi-stage differentiation defines melanoma subtypes with differential vulnerability to drug-induced iron-dependent oxidative stress. *Cancer Cell* **33**, 890–904.e5 (2018).
135. Graziani, V. et al. SLC7A11 protects amoeboid-disseminating cancer cells from oxidative stress. *Cell Rep.* **44**, 115939 (2025).

136. Schwab, A. et al. Zeb1 mediates EMT/plasticity-associated ferroptosis sensitivity in cancer cells by regulating lipogenic enzyme expression and phospholipid composition. *Nat. Cell Biol.* **26**, 1470–1481 (2024).
137. Tsai, F. et al. CD44-hyaluronan mediating endocytosis of iron-platinum alloy nanoparticles induces ferroptotic cell death in mesenchymal-state lung cancer cells with tyrosine kinase inhibitor resistance. *Acta Biomater.* **186**, 396–410 (2024).
138. Yang, F. et al. Ferroptosis heterogeneity in triple-negative breast cancer reveals an innovative immunotherapy combination strategy. *Cell Metab.* **35**, 84–100.e8 (2023).
139. Feng, J. et al. ACSL4 is a predictive biomarker of sorafenib sensitivity in hepatocellular carcinoma. *Acta Pharmacol. Sin.* **42**, 160–170 (2021).
140. Liang, D. et al. Ferroptosis surveillance independent of GPX4 and differentially regulated by sex hormones. *Cell* **186**, 2748–2764.e22 (2023).
141. Yan, H. et al. Discovery of decreased ferroptosis in male colorectal cancer patients with KRAS mutations. *Redox Biol.* **62**, 102699 (2023).
142. Liu, Z. et al. Systematic analysis of the aberrances and functional implications of ferroptosis in cancer. *iScience* **23**, 101302 (2020).
143. Zhu, Y. et al. Cancer-associated fibroblasts reprogram cysteine metabolism to increase tumor resistance to ferroptosis in pancreatic cancer. *Theranostics* **14**, 1683–1700 (2024).
144. Gurung, S. et al. Stromal lipid species dictate melanoma metastasis and tropism. *Cancer Cell* **43**, 1108–1124.e11 (2025).
145. Hecht, F. et al. Catabolism of extracellular glutathione supplies amino acids to support tumor growth. Preprint at [bioRxiv](https://doi.org/10.1101/2024.10.10.617667) <https://doi.org/10.1101/2024.10.10.617667> (2024).
146. Yang, Z. et al. HIF-1 α drives resistance to ferroptosis in solid tumors by promoting lactate production and activating SLC1A1. *Cell Rep.* **42**, 112945 (2023).
147. Chauhan, S. S. et al. Hypoxia induced lipid droplet accumulation promotes resistance to ferroptosis in prostate cancer. *Oncotarget* **16**, 532–544 (2025).
148. Fan, Z. et al. Hypoxia blocks ferroptosis of hepatocellular carcinoma via suppression of METTL14 triggered YTHDF2-dependent silencing of SLC7A11. *J. Cell Mol. Med.* **25**, 10197–10212 (2021).
149. Tan, S. K. et al. Obesity-dependent adipokine chemerin suppresses fatty acid oxidation to confer ferroptosis resistance. *Cancer Discov.* **11**, 2072–2093 (2021).
150. Yang, Z. et al. OGT/HIF-2 α axis promotes the progression of clear cell renal cell carcinoma and regulates its sensitivity to ferroptosis. *iScience* **26**, 108148 (2023).
151. Minikes, A. M. et al. HIF-independent oxygen sensing via KDM6A regulates ferroptosis. *Mol. Cell* **85**, 2973–2987.e6 (2025).
152. Song, J. et al. Hypoxia inhibits ferritinophagy-mediated ferroptosis in esophageal squamous cell carcinoma via the USP2-NCOA4 axis. *Oncogene* **43**, 2000–2014 (2024).
153. Alvarez, S. W. et al. NFS1 undergoes positive selection in lung tumours and protects cells from ferroptosis. *Nature* **551**, 639–643 (2017).
154. Dierge, E. et al. Peroxidation of n-3 and n-6 polyunsaturated fatty acids in the acidic tumor environment leads to ferroptosis-mediated anticancer effects. *Cell Metab.* **33**, 1701–1715.e5 (2021).
155. Song, X. et al. PDK4 dictates metabolic resistance to ferroptosis by suppressing pyruvate oxidation and fatty acid synthesis. *Cell Rep.* **34**, 108767 (2021).
156. Wen, Q., Liu, J., Kang, R., Zhou, B. & Tang, D. The release and activity of HMGB1 in ferroptosis. *Biochem. Biophys. Res. Commun.* **510**, 278–283 (2019).
157. Efimova, I. et al. Vaccination with early ferroptotic cancer cells induces efficient antitumor immunity. *J. Immunother. Cancer* **8**, e001369 (2020).
158. Liu, J. et al. DCN released from ferroptotic cells ignites AGER-dependent immune responses. *Autophagy* **18**, 2036–2049 (2022).
159. Morotti, M. et al. PGE₂ inhibits TIL expansion by disrupting IL-2 signalling and mitochondrial function. *Nature* **629**, 426–434 (2024).
160. Liu, J. et al. Extracellular GPX4 impairs antitumor immunity via dendritic ZP3 receptors. *Cell* **189**, 1056–1073 (2026).
161. Ma, X. et al. CD36-mediated ferroptosis dampens intratumoral CD8⁺ T cell effector function and impairs their antitumor ability. *Cell Metab.* **33**, 1001–1012.e5 (2021).
162. Han, L. et al. PPAR γ -mediated ferroptosis in dendritic cells limits antitumor immunity. *Biochem. Biophys. Res. Commun.* **576**, 33–39 (2021).
163. Wang, W. et al. CD8⁺ T cells regulate tumour ferroptosis during cancer immunotherapy. *Nature* **569**, 270–274 (2019).
164. Liao, P. et al. CD8⁺ T cells and fatty acids orchestrate tumor ferroptosis and immunity via ACSL4. *Cancer Cell* **40**, 365–378.e6 (2022).
165. Cui, W. et al. Gut microbial metabolite facilitates colorectal cancer development via ferroptosis inhibition. *Nat. Cell Biol.* **26**, 124–137 (2024).
166. Fiore, A. et al. Kynurenine importation by SLC7A11 propagates anti-ferroptotic signaling. *Mol. Cell* **82**, 920–932.e27 (2022).
167. Zitvogel, L., Fidelle, M. & Kroemer, G. Long-distance microbial mechanisms impacting cancer immunosurveillance. *Immunity* **57**, 2013–2029 (2024).
168. Jia, T. et al. A *Pseudomonas aeruginosa* quorum-sensing metabolite manipulates macrophage ferroptosis through a methylation pathway. *Nat. Commun.* **16**, 9992 (2025).
169. Dai, E. et al. Ferroptotic damage promotes pancreatic tumorigenesis through a TME173/STING-dependent DNA sensor pathway. *Nat. Commun.* **11**, 6339 (2020).
170. Rademaker, G. et al. PCSK9 drives sterol-dependent metastatic organ choice in pancreatic cancer. *Nature* **643**, 1381–1390 (2025).
171. Conche, C. et al. Combining ferroptosis induction with MDSC blockade renders primary tumours and metastases in liver sensitive to immune checkpoint blockade. *Gut* **72**, 1774–1782 (2023).
172. He, F. et al. ATF4 suppresses hepatocarcinogenesis by inducing SLC7A11 (xCT) to block stress-related ferroptosis. *J. Hepatol.* **79**, 362–377 (2023).
173. Guo, J. et al. The origin of hepatocellular carcinoma depends on metabolic zonation. *Science* **391**, eadv7129 (2025).
174. Ubellacker, J. M. et al. Lymph protects metastasizing melanoma cells from ferroptosis. *Nature* **585**, 113–118 (2020).
175. Hong, X. et al. The lipogenic regulator SREBP2 induces transferrin in circulating melanoma cells and suppresses ferroptosis. *Cancer Discov.* **11**, 678–695 (2021).
176. Wang, Y. et al. ACSL4 and polyunsaturated lipids support metastatic extravasation and colonization. *Cell* **188**, 412–429.e27 (2025).
177. Zhao, Z. et al. Sickle cell disease induces chromatin introversion and ferroptosis in CD8⁺ T cells to suppress anti-tumor immunity. *Immunity* **58**, 1484–1501.e11 (2025).
178. Morgan, P. K. et al. A lipid atlas of human and mouse immune cells provides insights into ferroptosis susceptibility. *Nat. Cell Biol.* **26**, 645–659 (2024).
179. Xu, S. et al. Uptake of oxidized lipids by the scavenger receptor CD36 promotes lipid peroxidation and dysfunction in CD8⁺ T cells in tumors. *Immunity* **54**, 1561–1577.e7 (2021).
180. Tzeng, S. F. et al. PLT012, a humanized CD36-blocking antibody, is effective for unleashing antitumor immunity against liver cancer and liver metastasis. *Cancer Discov.* **15**, 1676–1696 (2025).
181. Ping, Y. et al. PD-1 signaling limits expression of phospholipid phosphatase 1 and promotes intratumoral CD8⁺ T cell ferroptosis. *Immunity* **57**, 2122–2139.e9 (2024).
182. Xiao, L. et al. IL-9/STAT3/fatty acid oxidation-mediated lipid peroxidation contributes to Tc9 cell longevity and enhanced antitumor activity. *J. Clin. Invest.* **132**, e153247 (2022).
183. Xu, C. et al. The glutathione peroxidase Gpx4 prevents lipid peroxidation and ferroptosis to sustain Treg cell activation and suppression of antitumor immunity. *Cell Rep.* **35**, 109235 (2021).
184. Poznanski, S. M. et al. Metabolic flexibility determines human NK cell functional fate in the tumor microenvironment. *Cell Metab.* **33**, 1205–1220.e5 (2021).
185. Cui, J. X. et al. L-kynurenine induces NK cell loss in gastric cancer microenvironment via promoting ferroptosis. *J. Exp. Clin. Cancer Res.* **42**, 52 (2023).
186. Kim, R. et al. Ferroptosis of tumour neutrophils causes immune suppression in cancer. *Nature* **612**, 338–346 (2022).
187. Della Volpe, L. et al. Inhibiting ferroptosis enhances ex vivo expansion of human haematopoietic stem cells. *Nat. Cell Biol.* **27**, 2214–2224 (2025).
188. Zhao, J. et al. Human hematopoietic stem cell vulnerability to ferroptosis. *Cell* **186**, 732–747.e16 (2023).
189. Carlson, B. A. et al. Glutathione peroxidase 4 and vitamin E cooperatively prevent hepatocellular degeneration. *Redox Biol.* **9**, 22–31 (2016).
190. Ferrer, E. et al. Ketogenic diet promotes tumor ferroptosis but induces relative corticosterone deficiency that accelerates cachexia. *Cell Metab.* **35**, 1147–1162.e7 (2023).
191. Shi, L. et al. The DRD2 antagonist haloperidol mediates autophagy-induced ferroptosis to increase temozolomide sensitivity by promoting endoplasmic reticulum stress in glioblastoma. *Clin. Cancer Res.* **29**, 3172–3188 (2023).
192. Yue, J. et al. Discovery of the inhibitor targeting the SLC7A11/xCT axis through in silico and in vitro experiments. *Int. J. Mol. Sci.* **25**, 8284 (2024).
193. Cramer, S. L. et al. Systemic depletion of L-cyst(e)ine with cyst(e)inase increases reactive oxygen species and suppresses tumor growth. *Nat. Med.* **23**, 120–127 (2017).
194. Agnello, G. et al. Development of a human therapeutic L-cyst(e)ine-degrading enzyme for the treatment of hematological malignancies. *Blood* **128**, 1587–1587 (2016).
195. Guerra, A., Parhiz, H. & Rivella, S. Novel potential therapeutics to modify iron metabolism and red cell synthesis in diseases associated with defective erythropoiesis. *Haematologica* **108**, 2582–2593 (2023).
196. Liu, J., Tang, D. & Kang, R. Targeting GPX4 in ferroptosis and cancer: chemical strategies and challenges. *Trends Pharmacol. Sci.* **45**, 666–670 (2024).
197. Dai, Q. et al. Inhibition of FSP1: a new strategy for the treatment of tumors (Review). *Oncol. Rep.* **52**, 105 (2024).
198. Liu, H. et al. Small-molecule allosteric inhibitors of GPX4. *Cell Chem. Biol.* **29**, 1680–1693.e9 (2022).
199. Sun, D. et al. Simvastatin inhibits PD-L1 via ILF3 to induce ferroptosis in gastric cancer cells. *Cell Death Dis.* **16**, 208 (2025).
200. Li, J. et al. Tumor-specific GPX4 degradation enhances ferroptosis-initiated antitumor immune response in mouse models of pancreatic cancer. *Sci. Transl. Med.* **15**, eadg3049 (2023).
201. Wang, C. et al. Dual degradation mechanism of GPX4 degrader in induction of ferroptosis exerting anti-resistant tumor effect. *Eur. J. Med. Chem.* **247**, 115072 (2023).
202. Zhu, J. et al. PROTAC degraders of FSP1 act as potent GPX4 sensitizers to induce ferroptosis for hepatoma treatment. *Chin. Chem. Lett.* **37**, 11185 (2026).
203. Szwed, M., Poczta-Krawczyk, A., Bukowski, K. & Marczak, A. Nanoparticle-mediated ferroptosis for cancer therapy: mechanisms and therapeutic strategies. *Nanotechnol. Sci. Appl.* **18**, 445–470 (2025).
204. Huang, A. et al. An iron-containing nanomedicine for inducing deep tumor penetration and synergistic ferroptosis in enhanced pancreatic cancer therapy. *Mater. Today Bio* **27**, 101132 (2024).
205. Zhang, Y., Du, J., Cui, X., Ling, Y. & Tang, C. Development of a bispecific CDH17-GUCY2C ADC bearing the ferroptosis inducer RSL3 for the treatment of colorectal cancer. *Cell Death Discov.* **11**, 347 (2025).
206. Chung, T. T., Piao, Z. & Lee, S. J. Identification of ferroptosis-related signature predicting prognosis and therapeutic responses in pancreatic cancer. *Sci. Rep.* **15**, 75 (2025).
207. Wenzel, S. E. et al. PEBP1 warden ferroptosis by enabling lipoxygenase generation of lipid death signals. *Cell* **171**, 628–641.e6 (2017).

208. Minami, J. K. et al. CDKN2A deletion remodels lipid metabolism to prime glioblastoma for ferroptosis. *Cancer Cell* **41**, 1048–1060.e9 (2023).
209. Zhao, N. et al. Ferronostics: measuring tumoral ferrous iron with PET to predict sensitivity to iron-targeted cancer therapies. *J. Nucl. Med.* **62**, 949–955 (2021).
210. Shibata, Y., Yasui, H., Higashikawa, K. & Kuge, Y. Transferrin-based radiolabeled probe predicts the sensitivity of human renal cancer cell lines to ferroptosis inducer erastin. *Biochem. Biophys. Rep.* **26**, 100957 (2021).
211. Park, S. Y. et al. Clinical evaluation of (4S)-4-(3-[¹⁸F]fluoropropyl)-L-glutamate (¹⁸F-FSPG) for PET/CT imaging in patients with newly diagnosed and recurrent prostate cancer. *Clin. Cancer Res.* **26**, 5380–5387 (2020).
212. Park, S. Y. et al. Initial evaluation of (4S)-4-(3-[¹⁸F]fluoropropyl)-L-glutamate (FSPG) PET/CT imaging in patients with head and neck cancer, colorectal cancer, or non-Hodgkin lymphoma. *EJNMMI Res.* **10**, 100 (2020).
213. Zeng, F. et al. Ferroptosis MRI for early detection of anticancer drug-induced acute cardiac/kidney injuries. *Sci. Adv.* **9**, eadd8539 (2023).
214. Cui, S. et al. Identification of hyperoxidized PRDX3 as a ferroptosis marker reveals ferroptotic damage in chronic liver diseases. *Mol. Cell* **83**, 3931–3939 (2023).
215. Xu, S. et al. FXN targeting induces cell death in ovarian cancer stem-like cells through PRDX3-mediated oxidative stress. *iScience* **27**, 110506 (2024).
216. Jiang, Y. Z. et al. Integrated multiomic profiling of breast cancer in the Chinese population reveals patient stratification and therapeutic vulnerabilities. *Nat. Cancer* **5**, 673–690 (2024).
217. Tang, C. et al. Immunometabolic coevolution defines unique microenvironmental niches in ccRCC. *Cell Metab.* **35**, 1424–1440.e5 (2023).
218. Chen, R., Zou, J., Liu, J., Kang, R. & Tang, D. DAMPs in the immunogenicity of cell death. *Mol. Cell* **85**, 3874–3889 (2025).
219. Dai, E. et al. Autophagy-dependent ferroptosis drives tumor-associated macrophage polarization via release and uptake of oncogenic KRAS protein. *Autophagy* **16**, 2069–2083 (2020).
220. Xiao, Y. et al. HEBP2-governed glutamine competition between tumor and macrophages dictates immunotherapy efficacy in triple-negative breast cancer. *Cell Metab.* **37**, 2030–2047.e7 (2025).
221. Li, S. et al. Neutralization of acyl coenzyme A binding protein for the experimental prevention and treatment of hepatocellular carcinoma. *Cell Rep. Med.* **6**, 102232 (2025).
222. Lei, G. et al. The role of ferroptosis in ionizing radiation-induced cell death and tumor suppression. *Cell Res.* **30**, 146–162 (2020).
223. Lang, X. et al. Radiotherapy and immunotherapy promote tumoral lipid oxidation and ferroptosis via synergistic repression of SLC7A11. *Cancer Discov.* **9**, 1673–1685 (2019).
224. Jin, X. et al. High-dose ionizing radiation-induced ferroptosis leads to radiotherapy sensitization of nasopharyngeal carcinoma. *Radiother. Oncol.* **213**, 111166 (2025).
225. Mao, C. et al. Unraveling ETC complex I function in ferroptosis reveals a potential ferroptosis-inducing therapeutic strategy for LKB1-deficient cancers. *Mol. Cell* **84**, 1964–1979.e6 (2024).
226. Zhang, T. et al. Targeting histone deacetylase enhances the therapeutic effect of erastin-induced ferroptosis in EGFR-activating mutant lung adenocarcinoma. *Transl. Lung Cancer Res.* **10**, 1857–1872 (2021).
227. Lv, D. et al. EGFR promotes ALKBH5 nuclear retention to attenuate N6-methyladenosine and protect against ferroptosis in glioblastoma. *Mol. Cell* **83**, 4334–4351.e7 (2023).
228. Bian, Y. et al. Targeting ALDH1A1 to enhance the efficacy of KRAS-targeted therapy through ferroptosis. *Redox Biol.* **77**, 103361 (2024).
229. Bian, Y. et al. Targeting polyamine metabolism and ferroptosis enhances the efficacy of KRAS-targeted therapy depending on KEAP1 status. *Nat. Commun.* **16**, 9923 (2025).
230. Zheng, H. et al. Targeted activation of ferroptosis in colorectal cancer via LGR4 targeting overcomes acquired drug resistance. *Nat. Cancer* **5**, 572–589 (2024).
231. Guo, L., Hu, C., Yao, M. & Han, G. Mechanism of sorafenib resistance associated with ferroptosis in HCC. *Front. Pharmacol.* **14**, 1207496 (2023).
232. Bruedigam, C. et al. Imetelstat-mediated alterations in fatty acid metabolism to induce ferroptosis as a therapeutic strategy for acute myeloid leukemia. *Nat. Cancer* **5**, 47–65 (2024).
233. Sen, U., Coleman, C. & Sen, T. Stearoyl coenzyme A desaturase-1: multitasker in cancer, metabolism, and ferroptosis. *Trends Cancer* **9**, 480–489 (2023).
234. Sen, U. et al. SCD1 inhibition blocks the AKT-NRF2-SLC7A11 pathway to induce lipid metabolism remodeling and ferroptosis priming in lung adenocarcinoma. *Cancer Res.* **85**, 2485–2503 (2025).
235. Bartolacci, C. et al. Targeting de novo lipogenesis and the Lands cycle induces ferroptosis in KRAS-mutant lung cancer. *Nat. Commun.* **13**, 4327 (2022).
236. Chen, Y. et al. Mevalonate pathway promotes liver cancer by suppressing ferroptosis through CoQ10 production and selenocysteine-tRNA modification. *J. Hepatol.* **83**, 1338–1352 (2025).
237. Guo, D., Bell, E. H., Mischel, P. & Chakravarti, A. Targeting SREBP-1-driven lipid metabolism to treat cancer. *Curr. Pharm. Des.* **20**, 2619–2626 (2014).
238. Wong, T. L., Kong, Y. & Ma, S. Lipid metabolism in cancer cells: its role in hepatocellular carcinoma progression and therapeutic resistance. *Hepatol. Commun.* **9**, e0837 (2025).
239. Wang, X. et al. Adipocyte-derived ferroptotic signaling mitigates obesity. *Cell Metab.* **37**, 673–691.e7 (2025).
240. Dixon, S. J. et al. Pharmacological inhibition of cystine-glutamate exchange induces endoplasmic reticulum stress and ferroptosis. *eLife* **3**, e02523 (2014).
241. Zhu, S. et al. HSPA5 regulates ferroptotic cell death in cancer cells. *Cancer Res.* **77**, 2064–2077 (2017).
242. Fang, X. et al. Ferroptosis as a target for protection against cardiomyopathy. *Proc. Natl Acad. Sci. USA* **116**, 2672–2680 (2019).
243. Tadokoro, T. et al. Mitochondria-dependent ferroptosis plays a pivotal role in doxorubicin cardiotoxicity. *JCI Insight* **5**, e132747 (2020).
244. Xie, X. et al. Targeting GPX4-mediated ferroptosis protection sensitizes BRCA1-deficient cancer cells to PARP inhibitors. *Redox Biol.* **76**, 103350 (2024).
245. Chen, Z. et al. PRDX6 contributes to selenocysteine metabolism and ferroptosis resistance. *Mol. Cell* **84**, 4645–4659.e9 (2024).
246. Ito, J. et al. PRDX6 dictates ferroptosis sensitivity by directing cellular selenium utilization. *Mol. Cell* **84**, 4629–4644.e9 (2024).
247. Hu, Y. et al. Targeting PRDX6-dependent localization and function of GPX4 enhances ferroptosis-mediated tumor suppression. *Mol. Cell* **85**, 4602–4620.e9 (2025).
248. Tao, Y. et al. SCRNI confers hepatocellular carcinoma resistance to ferroptosis by stabilizing GPX4 via STK38-mediated phosphorylation. *Nat. Cancer* **6**, 1976–1993 (2025).
249. Wu, K. et al. Creatine kinase B suppresses ferroptosis by phosphorylating GPX4 through a moonlighting function. *Nat. Cell Biol.* **25**, 714–725 (2023).
250. Zhou, L. et al. Palmitoylation of GPX4 via the targetable ZDHHC8 determines ferroptosis sensitivity and antitumor immunity. *Nat. Cancer* **6**, 768–785 (2025).
251. Fan, Y. et al. PRMT5-mediated arginine methylation stabilizes GPX4 to suppress ferroptosis in cancer. *Nat. Cell Biol.* **27**, 641–653 (2025).

Acknowledgements

The authors thank the many pioneers in the field and colleagues whose work has shaped current understanding of ferroptosis.

Author contributions

D.T. conceived and supervised the overall framework of the Review. All authors contributed substantially to discussions of content, writing, and review and editing of all sections of the manuscript.

Competing interests

G.K. declares research contracts with Daiichi Sankyo, Eleor, Kaleido Biosciences, Lytx Pharma, PharmaMar, Osasuna Therapeutics, Samsara Therapeutics, Sanofi, Sutro Biopharma, Tollys and VAScage; serves on the Board of Directors of the Bristol Myers Squibb Foundation France, and on scientific advisory boards for Hevolution, Institut Servier, Longevity Vision Funds and Rejuvenon Life Sciences/Centenara Labs; is a scientific co-founder of everImmune, Osasuna Therapeutics, Samsara Therapeutics and Therafast Bio; and is the inventor of patents covering therapeutic targeting of ageing, cancer, cystic fibrosis and metabolic disorders, including one, ‘Methods for weight reduction’ (US11905330B1), relevant to this work. G.K.’s brother, Romano Kroemer, was an employee of Sanofi and now consults for Boehringer-Ingelheim. G.K.’s wife, Laurence Zitvogel, has held research contracts with GSK, Incyte, Lytx Pharma, Kaleido Biosciences, Innovate Pharma, Daiichi Sankyo, PiLeJe, Merus, Transgene SA, 9M Life Sciences, Tusk Therapeutic and Roche; was on the Board of Directors of Transgene SA; is a cofounder of everImmune; and holds patents covering the treatment of cancer and the therapeutic manipulation of the microbiota. The other authors declare no competing interests.

Additional information

Peer review information *Nature Reviews Clinical Oncology* thanks E. Catanzaro, X. Chen, F. Wang and the other, anonymous, reviewer(s) for their contribution to the peer review of this work.

Publisher’s note Springer Nature remains neutral with regard to jurisdictional claims in published maps and institutional affiliations.

Springer Nature or its licensor (e.g. a society or other partner) holds exclusive rights to this article under a publishing agreement with the author(s) or other rightsholder(s); author self-archiving of the accepted manuscript version of this article is solely governed by the terms of such publishing agreement and applicable law.

Related links

US NIH ClinicalTrials.gov database: <https://www.clinicaltrials.gov>

US NIH PubChem database: <https://pubchem.ncbi.nlm.nih.gov/>

© Springer Nature Limited 2026